

Even-odd effects in the $J_1 - J_2$ $SU(N)$ Heisenberg spin chain

L. Herviou,¹ S. Capponi,² and P. Lecheminant³

¹*Institute of Physics, Ecole Polytechnique Fédérale de Lausanne (EPFL), CH-105 Lausanne, Switzerland.*

²*Laboratoire de Physique Théorique, Université de Toulouse, CNRS, UPS, France.*

³*Laboratoire de Physique Théorique et Modélisation, CNRS, CY Cergy Paris Université, 95302 Cergy-Pontoise Cedex, France.*

(Dated: May 23, 2023)

The zero-temperature phase diagram of the $J_1 - J_2$ $SU(N)$ antiferromagnetic Heisenberg spin chain is investigated by means of complementary field theory and numerical approaches for general N . A fully gapped $SU(N)$ valence bond solid made of N sites is formed above a critical value of J_2/J_1 for all N . We find that the extension of this N -merized phase for larger values of J_2 strongly depends on the parity of N . For even N , the phase smoothly interpolates to the large J_2 regime where the model can be viewed as a zigzag $SU(N)$ two-leg spin ladder. The phase exhibits both a N -merized ground state and incommensurate spin-spin correlations. In stark contrast to the even case, we show that the N -merized phase with odd N has only a finite extent with no incommensuration. A gapless phase in the $SU(N)_1$ universality class is stabilized for larger J_2 that stems from the existence of a massless renormalization group flow from $SU(N)_2$ to $SU(N)_1$ conformal field theories when N is odd.

I. INTRODUCTION

Since the proposal made by Anderson,¹ a central focus of quantum magnetism over the years has been the study of the interplay between frustration and quantum fluctuations. Competing interactions or geometric frustration strongly enhance quantum fluctuations and the magnetic order can be destroyed by large low-energy excitations. As a result, novel quantum phases of matter, such as quantum spin liquids, can emerge in such systems.² Quantum fluctuations are also amplified by considering lattice spin systems with a larger $SU(N)$ internal symmetry than the $SU(2)$ spin rotation.³⁻⁵ Non-magnetic ground states are then more likely for large values of N since the extensive degeneracy in the semiclassical limit is larger. In this respect, large- N approaches on different two-dimensional $SU(N)$ spin models found a variety of non-Néel ground states as valence-bond solid (VBS) states and Abelian and non-Abelian chiral spin liquid ground states with topological order.^{3,4,6} The latter states are magnetic counterparts of the fractional quantum Hall phases and have excitations with fractional quantum numbers and fractional statistics or non-Abelian ones. For smaller values of N ($3 \leq N \leq 10$), numerical and variational approaches have identified chiral and algebraic spin liquids ground states in various two-dimensional $SU(N)$ quantum magnets.⁷⁻¹² In one dimension, the $SU(N)$ symmetry also plays a key role by stabilising exotic symmetry protected topological phases which are beyond the $SU(2)$ case.¹³⁻¹⁹

The simplest model to analyze the interplay between frustration and an $SU(N)$ symmetry in one dimension is the $J_1 - J_2$ antiferromagnetic $SU(N)$ Heisenberg spin chain with Hamiltonian:

$$H_{J_1 - J_2} = J_1 \sum_{i,A} S_i^A S_{i+1}^A + J_2 \sum_{i,A} S_i^A S_{i+2}^A, \quad (1)$$

where S_i^A ($A = 1, \dots, N^2 - 1$) denotes the $SU(N)$ spin operators on the i th site of the chain which transform in the fundamental representation N of the $SU(N)$ group. These spin operators are normalized as $\text{Tr}(S^A S^B) = \delta^{AB}/2$ and

the spin exchanges are antiferromagnetic ($J_{1,2} \geq 0$). Model (1) can be realized by loading ultracold fermionic alkaline-earth or ytterbium atoms in a zigzag optical lattice as in Ref. 20 and driving them into the Mott-insulating regime with one atom per site. With the considerable progress made in ultracold $SU(N)$ fermionic experiments,²¹⁻²⁶ the $J_1 - J_2$ $SU(N)$ Heisenberg spin chain could be achieved in the near future.

The phase diagram of model (1) is well-known for $N = 2$ and the main effect of the competing J_2 interaction is to produce a Kosterlitz-Thouless transition between the critical phase of the spin-1/2 Heisenberg chain and a spontaneously dimerized phase.²⁷ In the presence of frustration, quantum fluctuations destroy the quasi-long-range order of a spin-1/2 Heisenberg chain by producing a spectral gap and the system dimerizes as exemplified by the exactly soluble Majumdar-Ghosh point when $J_2 = J_1/2$.²⁸ The ground state is two-fold degenerate and can be viewed as a valence bond solid made of two spins, breaking spontaneously the one-step translation symmetry T_{a_0} . The dimerized phase is stabilized when $J_2/J_1 \geq 0.2411$.²⁹ The gapless spinons of the spin-1/2 Heisenberg chain with fractional $S = 1/2$ quantum numbers becomes fully gapped in the dimerized phase. They are still deconfined excitations and can be viewed as the domain walls between the two-degenerate ground states.³⁰ This dimerized phase extends to the strong J_2 regime where the $J_1 - J_2$ Heisenberg spin chain (1) can be viewed as a two-leg spin ladder with a triangular or zigzag geometry.³¹⁻³⁴

In stark contrast to $N = 2$, little is known for the phase diagram of model (1) for general $N > 2$ even in the large N limit. When $J_2 = 0$, model (1), e.g. the $SU(N)$ Heisenberg spin chain, is the so-called Sutherland model which is integrable by means of Bethe ansatz.³⁵ It displays a quantum critical behavior in the $SU(N)_1$ Wess-Zumino-Novikov-Witten (WZNW) universality class with central charge $c = N - 1$.^{36,37} The predictions of the exact solution and of the conformal field theory (CFT) approach have been carefully checked numerically by means of various methods.³⁸⁻⁴⁵ The low-lying gapless excitations occur in pairs with individual dispersion relations covering a fraction of the Brillouin zone.⁴⁶ The elementary excita-

tions of the model are then a generalization of the spinons of the spin-1/2 Heisenberg chain and carry fractional quantum numbers. They transform in the conjugate \bar{N} representation of the $SU(N)$ group and, in this respect, they may be viewed as an analog of antiquarks in quantum chromodynamics.^{47,48} It has been shown that they display fractional statistics with angle $\theta = \pi/N$.⁴⁷⁻⁴⁹

What happens for these spinons excitations upon switching on a nonzero J_2 when $N > 2$? The lesson gained from the $N = 2$ case leads us to expect that the natural instability of the gapless phase with $c = N - 1$ is the formation of a singlet cluster phase of N sites, a N -merized phase. The latter is the natural generalization of the valence bond solid of $N = 2$, since N is the minimum number of spins needed to form an $SU(N)$ singlet for spins in the fundamental representation of the $SU(N)$ group. The $J_1 - J_2$ $SU(3)$ spin chain model has been investigated numerically by means of the density-matrix renormalization group (DMRG) and exact diagonalizations (EDs). A spontaneous trimerized phase, a singlet cluster phase of three sites, has been revealed when $0.45 \leq J_2/J_1 \leq 3.5$.⁵⁰ The phase is threefold degenerate and breaks spontaneously T_{a_0} . The generalized spinons become massive deconfined excitations which correspond to the domain walls of the trimerized phase similarly to the $N = 2$ case.^{49,51,52} Interestingly enough, it was found numerically that the trimerized phase has a finite extent and does not extend to the large J_2 regime in stark contrast to the $N = 2$ case.⁵⁰ A critical $SU(3)_1$ phase with $c = 2$ is expected to show up with deconfined critical spinons at sufficiently large J_2 .

In this paper, we map out the phase diagram of model (1) at zero temperature by means of complementary CFT techniques for $N > 2$ and numerical approaches ED and infinite size DMRG (iDMRG) for $N = 3, 4$. At intermediate J_2 for all N , we find the existence of a N -merized phase which is N -fold degenerate and breaks spontaneously T_{a_0} . The domain-wall excitations between consecutive degenerate ground states, i.e. N -merization kinks, have fractional quantum numbers and correspond to the deconfined gapped $SU(N)$ spinons which transform in the \bar{N} -representation of $SU(N)$. The extension of the N -merized phase in the large J_2 regime can be investigated numerically for $N = 3$ and $N = 4$ as well as by a field theory approach which exploits the existence of a decoupling critical point when $J_2 \rightarrow \infty$. In this large J_2 regime, the model is best visualized as a two-leg zigzag spin ladder where the J_1 bonds couple two $SU(N)$ Heisenberg spin chains with spin-exchange J_2 :

$$H_{\text{zigzag}} = J_2 \sum_{i,A} (S_{1,i}^A S_{1,i+1}^A + S_{2,i}^A S_{2,i+1}^A) + J_1 \sum_{i,A} S_{2,i}^A (S_{1,i}^A + S_{1,i+1}^A), \quad (2)$$

where $S_{1,i}^A$ and $S_{2,i}^A$ ($A = 1, \dots, N^2 - 1$) denote the $SU(N)$ spin operators on the i th site on the chains 1 and 2 which transform in the fundamental representation N of the $SU(N)$ group. The field theory analysis of the two-leg $SU(N)$ zigzag spin ladder (2) in the regime $J_1 \ll J_2$ reveals that the extension of the N -merized phase strongly depends on the parity of

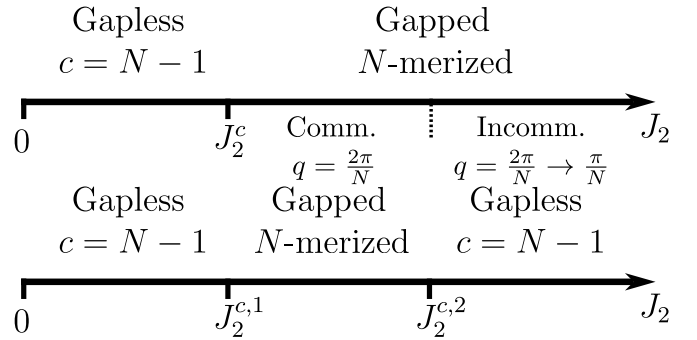


FIG. 1. Phase diagrams

N . In the odd N case, the existence of a massless renormalization group (RG) flow from $SU(N)_2$ to $SU(N)_1$ CFTs leads to the emergence of a gapless phase with $SU(N)_1$ quantum criticality when $J_1 \ll J_2$. The N -merized phase has thus a finite extent $J_2^{c,1} \leq J_2 \leq J_2^{c,2}$, surrounded by two $SU(N)_1$ gapless phases when N is odd. The original spinons of the Sutherland model experience a sequence of two transitions. A first one at $J_2 = J_2^{c,1}$, where they become fully gapped deconfined excitations in the N -merized phase and then at $J_2 = J_2^{c,2}$, where the gap closes and the spinons again become gapless. In contrast, the situation is very different in the even N case. We show analytically and numerically for $N = 4$ that the tetramerized phase smoothly interpolates to the strong-coupling large J_2 regime. In addition, we find that this phase for $J_2 > 2J_1$ is characterized by an incommensurate behavior in the spin-spin correlation function as in the $N = 2$ case whereas no such incommensuration is obtained for $N = 3$. Our conjectured phase diagrams are summarized in Fig. 1.

The paper is organized as follows. The low-energy approach appropriate in the weak-coupling region $J_2 \ll J_1$ and in the strong-coupling one $J_1 \ll J_2$ is presented in Sec. II. The results of extensive ED and DMRG calculations in the $N = 3$ and $N = 4$ cases are described in Sec. III. Finally, a summary of the main results is given in Sec. IV together with five technical appendixes.

II. LOW-ENERGY DESCRIPTION

The phase diagram of model (1) is investigated by a low-energy field theory approach using two different limits: the weak-coupling regime when $J_2 \ll J_1$ and the strong-coupling case $J_1 \ll J_2$ using the two-leg zigzag ladder geometry (2).

A. Weak-coupling regime: $J_2 \ll J_1$

Let us first consider the weak-coupling limit $J_2 \ll J_1$ by considering model (1). When $J_2 = 0$, the Sutherland model (1) displays a gapless behavior which is described by the $SU(N)_1$ CFT perturbed by a marginally irrelevant current-

current interaction with Hamiltonian density:^{36,37}

$$\mathcal{H}_{\text{sutherland}} = \frac{2\pi v}{N+1} (: J_R^A J_R^A : + : J_L^A J_L^A :) - \gamma J_R^A J_L^A, \quad (3)$$

where v is the spin velocity and $J_{L,R}^A$ are the left and right $SU(N)_1$ currents. In Eq. (3), a summation over repeated indices $A = 1, \dots, N^2 - 1$ is assumed as in the following. In the low-energy limit, a $SU(N)_1$ quantum critical behavior with a central charge $c = N - 1$ is stabilized and the marginally irrelevant current-current interaction ($\gamma > 0$) leads to logarithmic corrections in correlation functions.^{53–55}

The effect of the J_2 interaction of model (1) can be investigated in the weak-coupling limit since the lattice $SU(N)$ operators in the low-energy limit can be expressed in terms of the fields of the $SU(N)_1$ CFT as:^{37,39,56}

$$S_n^A/a_0 \simeq J_L^A + J_R^A + (e^{i2k_F x} N^A + \text{H.c.}) + \sum_{m=2}^{N-2} e^{i2mk_F x} n_m^A, \quad (4)$$

where $k_F = \pi/Na_0$, $x = na_0$, a_0 being the lattice spacing. The $2k_F$ part of the $SU(N)$ spin density involves the $SU(N)_1$ WZNW field g with scaling dimension $(N - 1)/N$ which transforms in the N -representation of the $SU(N)$ group:

$$N^A = iC \text{Tr}(gT^A), \quad (5)$$

C being a nonuniversal real constant and T^A are the generators in the N -representation normalized as: $\text{Tr}(T^A T^B) = \delta^{AB}/2$. The remaining $2mk_F$ parts of the decomposition (4) are related to the $m = 2, \dots, N - 2$ $SU(N)_1$ primary fields Φ_m with scaling dimension $m(N - m)/N$ which transform in the fully antisymmetric representation of $SU(N)$ made of a Young tableau with a single column and m lines:

$$n_m^A = i\alpha_m \text{Tr}(\Phi_m T_m^A), \quad (6)$$

where T_m^A are $SU(N)$ generators in the m th fully antisymmetric representation of the $SU(N)$ group and α_m are nonuniversal real constants. The $2mk_F$ component of the spin-density (4) satisfies the constraint: $n_m^{A\dagger} = n_{N-m}^A$.

Using the low-energy description (4), one can derive the continuum limit of model (1) in the weak-coupling regime $J_2 \ll J_1$. Its Hamiltonian density reads:

$$\mathcal{H}_{J_1-J_2} = \frac{2\pi v}{N+1} (: J_R^A J_R^A : + : J_L^A J_L^A :) + \lambda J_R^A J_L^A, \quad (7)$$

where $\lambda \simeq 2a_0 J_2 - \gamma$. Model (7) is an integrable field theory and its low-energy properties are well known.^{56,57} When $\lambda < 0$, the interaction is marginally irrelevant and it scales to zero in the far infrared (IR) limit so that the $SU(N)_1$ gapless phase of the Sutherland model extends to nonzero J_2 . In contrast, when $\lambda > 0$, a spectral gap is formed and the low-energy excitations are fully gapped. The nature of the phase can be determined by means of the continuum description of the N -merization operator (see for instance Appendix B of Ref. 58):

$$e^{-i\frac{2\pi n}{N}} S_n^A S_{n+1}^A \sim \text{Tr}_g(x). \quad (8)$$

In the fully gapped phase, one has $\langle \text{Tr}_g \rangle \neq 0$ and a N -merized phase is stabilized which is N -fold degenerate, breaking spontaneously T_{a_0} since according to the identifications 4 and 5:

$$g \rightarrow e^{i\frac{2\pi}{N}g}, \quad (9)$$

under T_{a_0} .

The existence of the N -merized phase can also be obtained by a direct Abelian-bosonization approach of model (7) as shown in Appendix A. Physically, the lattice spins form $SU(N)$ singlets and since N sites are needed to get an $SU(N)$ singlet, a N -merized phase or valence cluster phase of N sites emerges when $J_2 > J_2^{c,1}$ (e.g. $\lambda > 0$). The nonuniversal value $J_2^{c,1}$ of the transition cannot be determined within this low-energy approach and will be obtained by means of numerical approaches for $N = 3$ and $N = 4$ in Sec. III. The original gapless spinons of the Sutherland model when $J_2 = 0$ become fully gapped. As discussed in Appendix A, they correspond to the domain-wall configurations between the N -degenerate ground states of the N -merized phase. It is shown that they transform in the \bar{N} representation of the $SU(N)$ group and thus share the same quantum numbers as the $SU(N)$ gapless spinons of the Sutherland model.

B. Zigzag limit: $J_1 \ll J_2$

We now consider the opposite limit $J_1 \ll J_2$. A low-energy approach can still be derived by considering the $J_1 - J_2$ spin chain (1) as a zigzag two-leg spin ladder with Hamiltonian (2).

When $J_1 = 0$, we have two decoupled Sutherland models with central charge $c = 2(N - 1)$. A continuum limit can be performed by introducing two independent copies of the identification (4):

$$S_{l,n}^A \simeq J_{lL}^A + J_{lR}^A + (e^{i2k_F x} N_l^A + \text{H.c.}) + \sum_{m=2}^{N-2} e^{i2mk_F x} n_{lm}^A, \quad (10)$$

with $l = 1, 2$ and $x = na_0$. We introduce a small J_1 term which couples the two $SU(N)$ Sutherland models. Using Eq. (10), the leading part of the continuum limit of the J_1 term of the zigzag ladder Hamiltonian (2) reads then as follows by keeping only nonoscillatory terms:

$$\begin{aligned} \mathcal{H}_{\text{cont}}^{\text{zigzag}} &\simeq J_1 a_0 \left[e^{2ik_F x} N_2^A(x) + e^{-2ik_F x} N_2^{A\dagger}(x) \right] \\ &\quad \left[e^{2ik_F x} N_1^A(x) (1 + e^{2ik_F a_0}) + \text{H.c.} \right] \\ &= 2a_0 J_1 \cos\left(\frac{\pi}{N}\right) \left(e^{i\pi/N} N_1^A N_2^{A\dagger} + \text{H.c.} \right). \quad (11) \end{aligned}$$

In strong contrast to the $N = 2$ case, the $2k_F$ backscattering for $N > 2$ terms do not cancel exactly.^{31,32} In this respect, the situation is very different from the $N = 2$ case where the leading perturbation is only marginal with a twist perturbation with nonzero conformal spin and current-current interactions.³³ The interaction is now strongly relevant. By exploiting the fact that N_l^A can be expressed in terms of

the two $SU(N)_1$ WZNW fields $g_{1,2}$ with scaling dimension $(N-1)/N$:

$$N_l^A = iC \text{Tr}(g_l T^A), \quad (12)$$

we get the leading part of the low-energy effective theory which governs the IR behavior of model (2) in the regime $J_1 \ll J_2$:

$$\begin{aligned} \mathcal{H}_{\text{zigzag}} &= \frac{2\pi v}{N+1} \sum_{l=1}^2 (: J_{lR}^A J_{lR}^A : + : J_{lL}^A J_{lL}^A :) \\ &+ \lambda_1 \left[e^{i\pi/N} \text{Tr}(g_1 g_2^\dagger) + \text{H.c.} \right] \\ &+ \lambda_2 \left[e^{i\pi/N} \text{Tr} g_1 \text{Tr} g_2^\dagger + \text{H.c.} \right], \end{aligned} \quad (13)$$

where $\lambda_2 = -\lambda_1/N < 0$ and $\lambda_1 = a_0 J_1 C^2 \cos(\pi/N) > 0$.

Model (13) describes two $SU(N)_1$ WZNW models perturbed by two strongly relevant perturbations with the same scaling dimension $2(N-1)/N < 2$ which are expected to open a spectral gap $\Delta \sim J_1^{N/2}$ (up to logarithmic corrections) as soon as the inter-chain coupling J_1 is switched on (the gap opens more slowly for larger N). The subdominant contribution to model (13) corresponds to the marginal current-current interaction:

$$\mathcal{H}_{cc} = \frac{1}{2} (J_1 - \gamma) I_R^A I_L^A - \frac{1}{2} (J_1 + \gamma) K_R^A K_L^A, \quad (14)$$

where $I_{R,L}^A = J_{1R,L}^A + J_{2R,L}^A$ is a $SU(N)_2$ current, being the sum of two $SU(N)_1$ currents, and $K_{R,L}^A = J_{1R,L}^A - J_{2R,L}^A$ is the so-called wrong current.⁵⁹ In the $N=4$ case, there is an additional marginal contribution which stems from the product $n_{12}^A n_{22}^A$.

The effective Hamiltonian density (13) and the marginal contribution (14) thus describe the low-energy physics of the two-leg zigzag $SU(N)$ spin ladder (2) in the regime $J_1 \ll J_2$. It takes a rather similar form from the one obtained in Refs. 58 and 60 for the standard two-leg $SU(N)$ spin ladder, e.g. with a rectangular symmetry. However, there is a crucial difference here with the presence of the phase factor $e^{i\pi/N}$ in Eq. (13), stemming from the zigzag geometry, which makes the physics totally different.

The next step of the approach to elucidate the IR properties of model (13) is to exploit the existence of the following conformal embedding as in Refs. 58, 60, and 61:

$$SU(N)_1 \times SU(N)_1 \sim SU(N)_2 \times \mathbb{Z}_N, \quad (15)$$

where \mathbb{Z}_N is the parafermionic CFT with central charge $c = 2(N-1)/(N+2)$ which describes the universal properties of the phase transition of the two-dimensional \mathbb{Z}_N clock model.⁶² The low-temperature phase of the latter model is described by local order parameters σ_k ($k = 1, \dots, N-1$) which are primary fields of the \mathbb{Z}_N CFT with scaling dimension $d_k = k(N-k)/N(N+2)$. The $SU(N)_2$ CFT has the central charge $c = 2(N^2-1)/(N+2)$ and is generated by the currents $I_{R,L}^A$. The two $SU(N)_1$ WZNW fields $g_{1,2}$ can be expressed in the new $SU(N)_2 \times \mathbb{Z}_N$ basis as:^{58,63}

$$\begin{aligned} (g_1)_{\alpha\beta} &\sim G_{\alpha\beta} \sigma_1 \\ (g_2)_{\alpha\beta} &\sim G_{\alpha\beta} \sigma_1^\dagger, \end{aligned} \quad (16)$$

where $\alpha, \beta = 1, \dots, N$ and G is the $SU(N)_2$ WZNW field (in N -representation) with scaling dimension $\Delta_G = (N^2-1)/N(N+2)$.⁶⁴ Under T_{a_0} , $g_{1,2} \rightarrow e^{i\frac{2\pi}{N}} g_{1,2}$ as in Eq. (9) so that one has from (16)

$$G \rightarrow e^{i\frac{2\pi}{N}} G, \quad (17)$$

under T_{a_0} .

Using the Appendix B (see also Ref. 58), model (13) can be expressed in the new basis (15) as:

$$\begin{aligned} \mathcal{H}_{\text{zigzag}} &= \frac{2\pi v}{N+2} (: I_R^A I_R^A : + : I_L^A I_L^A :) + \mathcal{H}_{\mathbb{Z}_N} \\ &+ \tilde{\lambda}_1 \left(e^{i\pi/N} \Psi_{1L} \Psi_{1R} + \text{H.c.} \right) \\ &+ \tilde{\lambda}_2 \text{Tr}(\Phi_{\text{adj}}) \left(e^{i\pi/N} \sigma_2 + \text{H.c.} \right), \end{aligned} \quad (18)$$

where $\mathcal{H}_{\mathbb{Z}_N}$ is the Hamiltonian density of the \mathbb{Z}_N parafermionic CFT. The latter is generated by the first \mathbb{Z}_N parafermion currents $\Psi_{1L,R}$ with conformal weights $h, \bar{h} = (N-1)/N$. In Eq. (18), Φ_{adj} is the $SU(N)_2$ primary field with scaling dimension $2N/(N+2)$, which transforms in the adjoint representation of $SU(N)$ and the coupling constants are given by:

$$\begin{aligned} \tilde{\lambda}_1 &= \frac{(N^2-1)\lambda_1}{N} = a_0 \frac{(N^2-1)}{N} J_1 C^2 \cos(\pi/N) > 0 \\ \tilde{\lambda}_2 &= \lambda_2 = -a_0 J_1 C^2 \frac{\cos(\pi/N)}{N} < 0. \end{aligned} \quad (19)$$

The effective field theory (18) contains two different sectors, an $SU(N)$ singlet one, described by the \mathbb{Z}_N parafermions, and the second one depending on both $SU(N)$ and \mathbb{Z}_N degrees of freedom. The two perturbations are strongly relevant with the same scaling dimension. Interestingly, the pure \mathbb{Z}_N perturbation with coupling constant $\tilde{\lambda}_1$ in Eq. (18) is an integrable field theory.⁶⁵ Its Euclidean action is given by

$$\mathcal{S}_{\text{eff}} = \mathcal{S}_{\mathbb{Z}_N} - g \int d^2x \left(e^{i\pi/N} \Psi_{1L} \Psi_{1R} + \text{H.c.} \right), \quad (20)$$

where $\mathcal{S}_{\mathbb{Z}_N}$ is the action of the \mathbb{Z}_N CFT and $g = -\tilde{\lambda}_1 < 0$. The IR properties of the action (20) strongly depend on the sign of the coupling constant g and of the parity of N .⁶⁵ When $g > 0$, \mathcal{S}_{eff} displays an integrable massless RG flow to the minimal model series \mathcal{M}_{N+1} with central charge $c = 1 - 6/(N+1)(N+2)$.⁶⁵ When $g < 0$, as is the case here since $J_1 > 0$, the IR behavior depends on the parity of N . When N is even, the minus sign of the perturbation in Eq. (20) can be absorbed into a redefinition of the first parafermionic current: $\Psi_{1L} \rightarrow -\Psi_{1L}$ which still satisfies the same parafermionic algebra. This means that \mathcal{S}_{eff} exhibits a massless RG flow to the minimal model series \mathcal{M}_{N+1} in the far-IR when $g < 0$ and N even. However, when N is odd, one cannot use the same transformation but the following redefinition:

$$\begin{aligned} \Psi_{1L} &\rightarrow \tilde{\Psi}_{1L} = -e^{i\pi/N} \Psi_{1L} \\ \Psi_{1R} &\rightarrow \tilde{\Psi}_{1R} = \Psi_{1R}, \end{aligned} \quad (21)$$

and $\tilde{\Psi}_{1L}$ is still a first parafermionic current ($\tilde{\Psi}_{1L}^N \sim I$) when N is odd. The action (20) transforms then as follows:

$$\mathcal{S}_{\text{eff}} = \mathcal{S}_{\mathbb{Z}_N} + g \int d^2x \left(\tilde{\Psi}_{1L} \tilde{\Psi}_{1R} + \text{H.c.} \right), \quad (22)$$

which is known to be a massive integrable field theory of \mathbb{Z}_N parafermions when $g = -\tilde{\lambda}_1 < 0$.⁶⁶ We thus conclude that the \mathbb{Z}_N perturbation (20) when $g < 0$, e.g. $J_1 > 0$, displays different physical properties depending on the parity of N . When N is even, model (20) is gapless in the long-distance limit with critical properties that are governed by the \mathcal{M}_{N+1} universality class while it is fully massive in the odd N case.

1. Odd- N case

We first focus on the odd- N case where model (20) is a massive field theory with a mass gap $\Delta \sim J_1^{N/2}$. The exact spectrum consists of massive kink excitations that result from degenerate ground states labeled by an odd integer $s = 1, 3, \dots, N$.⁶⁶ After averaging over the \mathbb{Z}_N degrees of freedom in Eq. (18), we obtain an effective theory for the remaining $\text{SU}(N)_2$ degrees of freedom that governs the physics of model (18) at the energy scale $E \ll \Delta$:

$$\mathcal{H}_{\text{eff}}^{\text{odd}} = \frac{2\pi v}{N+2} \left(: I_R^A I_R^A : + : I_L^A I_L^A : \right) + \tilde{\lambda}_2 \text{Tr}(\Phi_{\text{adj}}) \left(e^{i\pi/N} \langle \sigma_2 \rangle + \text{H.c.} \right). \quad (23)$$

The vacuum expectation value $\langle \sigma_k \rangle$ of the \mathbb{Z}_N spin operators in the field theory (22) with $g < 0$ have been determined nonperturbatively in Ref. 67. To use their result, we need to find the transformation of σ_2 under (21). By fusion, the transformation of the \mathbb{Z}_N parafermion currents ($\Psi_{kL,R}$, $k = 1, \dots, N-1$) is found to be:

$$\begin{aligned} \Psi_{kL} &\rightarrow \tilde{\Psi}_{kL} = (-1)^k e^{ik\pi/N} \Psi_{kL} \\ \Psi_{kR} &\rightarrow \tilde{\Psi}_{kR} = \Psi_{kR}. \end{aligned} \quad (24)$$

The transformation of the \mathbb{Z}_N spin fields σ_k should be consistent with the fusion rules of the \mathbb{Z}_N parafermionic theory:⁶² $\sigma_k \mu_k \sim \Psi_{kL}$ and $\sigma_k \mu_k^\dagger \sim \Psi_{kR}$ (μ_k being the \mathbb{Z}_N disorder fields). We thus deduce:

$$\begin{aligned} \sigma_2 &\rightarrow \tilde{\sigma}_2 = -e^{i\pi/N} \sigma_2 \\ \mu_2 &\rightarrow \tilde{\mu}_2 = -e^{i\pi/N} \mu_2. \end{aligned} \quad (25)$$

After the transformation (21), the low-energy Hamiltonian (23) becomes then

$$\begin{aligned} \mathcal{H}_{\text{eff}}^{\text{odd}} &= \frac{2\pi v}{N+2} \left(: I_R^A I_R^A : + : I_L^A I_L^A : \right) \\ &- \tilde{\lambda}_2 \text{Tr}(\Phi_{\text{adj}}) \left(\langle \tilde{\sigma}_2 \rangle + \text{H.c.} \right). \end{aligned} \quad (26)$$

The value $\langle \tilde{\sigma}_2 \rangle$ in the field theory (22) can be found in Ref. 67 and we find $\langle \tilde{\sigma}_2 \rangle = \langle \tilde{\sigma}_2^\dagger \rangle = \sigma > 0$.

Finally, the low-energy effective theory which governs the IR behavior of the two-leg $\text{SU}(N)$ zigzag spin ladder in the large J_2 limit reads as follows when N is odd:

$$\mathcal{H}_{\text{eff}}^{\text{odd}} = \frac{2\pi v}{N+2} \left(: I_R^A I_R^A : + : I_L^A I_L^A : \right) + \eta \text{Tr}(\Phi_{\text{adj}}), \quad (27)$$

with $\eta = -2\tilde{\lambda}_2\sigma > 0$. The effective field theory (27) has been investigated in Ref. 68. While the adjoint perturbation is a strongly relevant perturbation with scaling dimension $2N/(N+2)$, a massless RG flow from $\text{SU}(N)_2$ to $\text{SU}(N)_1$ CFT is predicted when N is odd and $\eta > 0$. An explicit proof in the $N = 3$ case has been given in Ref. 68 by mapping model (27) with $N = 3$ onto Gepner's parafermions,⁶⁹ and recently using RG interfaces.⁷⁰

We thus find that the two-leg $\text{SU}(N)$ zigzag spin ladder in the regime $J_1 \ll J_2$ displays critical properties in the $\text{SU}(N)_1$ universality class when N is odd as in the weak-coupling regime $J_2 \ll J_1$. An alternative approach in the $N = 3$ case, based on a semiclassical approach, is presented in Appendix C which confirms the existence of this $\text{SU}(3)_1$ gapless phase in the zigzag regime. The fully gapped N -merized phase, found in the weak-coupling regime $J_2 \ll J_1$, has thus a finite extent as function of J_2 when N is odd. The precise extension of this phase is clearly beyond the scope of the field-theory approach and will be investigated numerically in Sec. III. The transition between the $\text{SU}(N)_1$ phase, obtained in the regime $J_2 \gg J_1$, and the N -merized phase is similar to the one described in the weak-coupling regime $J_2 \ll J_1$. Along the massless RG flow, the $\text{SU}(N)_2$ currents $I_{L,R}^A$ are transmuted in the far-IR regime to $\text{SU}(N)_1$ currents $\mathcal{J}_{L,R}^A$ so that, taking into account the marginal contribution (14), the transition is expected to be governed by

$$\mathcal{H}_{\text{IR}}^{\text{odd}} = \frac{2\pi v}{N+1} \left(: \mathcal{J}_R^A \mathcal{J}_R^A : + : \mathcal{J}_L^A \mathcal{J}_L^A : \right) + \lambda_{\text{eff}} \mathcal{J}_R^A \mathcal{J}_L^A, \quad (28)$$

where $\lambda_{\text{eff}} < 0$ in the regime $J_2 \gg J_1$ and should change its sign at the transition to produce the fully gapped N -merized phase with an N -fold ground-state degeneracy.

2. Even- N case

We now turn to the even- N case. In stark contrast to the odd- N case, the \mathbb{Z}_N field theory (20) is not fully massive but describe an integrable massless RG flow to the minimal model series \mathcal{M}_{N+1} with central charge $c = 1 - 6/(N+1)(N+2)$. Along the RG flow, some \mathbb{Z}_N degrees of freedom acquire a gap but others remain gapless in the long-distance limit. It is thus tempting to expect that the physical properties of the two-leg $\text{SU}(N)$ zigzag ladder (2) for even N will be rather different from the odd N case.

The strategy for even N is thus to rewrite model (18) in the IR limit by exploiting the existence of the integrable massless RG flow. To this end, we need the ultraviolet (UV)-IR transmutation of the \mathbb{Z}_N fields and most importantly the expression of the order fields $\sigma_{1,2}$ at the IR \mathcal{M}_{N+1} fixed point. Unfortunately, to the best of our knowledge, we are not aware of such

UV-IR transmutation when $N > 4$. In the special $N = 4$ case, progress can be made by exploiting the fact that the \mathbb{Z}_4 CFT has central charge $c = 1$ and it can be described by a bosonic field Φ on the orbifold line.⁷¹ The field theory (20) turns out to be equivalent to the self-dual sine-Gordon model at $\beta^2 = 6\pi$ with Hamiltonian density:⁷¹

$$\mathcal{H}_{\text{SDSG}} = \frac{v}{2} \left[(\partial_x \Phi)^2 + (\partial_x \Theta)^2 \right] + g \left[\cos(\sqrt{6\pi} \Phi) + \cos(\sqrt{6\pi} \Theta) \right], \quad (29)$$

where Θ is the dual field associated with Φ . Model (29) is self-dual, being invariant under the $\Phi \leftrightarrow \Theta$ symmetry, with two strongly relevant perturbations with scaling dimension $3/2$. This self-duality symmetry produces a quantum critical behavior. Its nature can be inferred from the equivalence between (29) and the \mathbb{Z}_4 field theory (20) which displays a massless RG flow from the $c = 1$ \mathbb{Z}_4 CFT to the minimal model \mathcal{M}_5 with central charge $c = 4/5$. Model (29) enjoys thus a $c = 4/5$ quantum critical behavior. The σ_2 primary field of the \mathbb{Z}_4 CFT with scaling dimension $1/6$ can be bosonized and one has:⁷¹ $\sigma_2 = \sqrt{2} \cos(\sqrt{2\pi/3} \Phi)$. The low-energy effective field theory (18) reads then as follows for $N = 4$:

$$\mathcal{H}_{\text{zigzag}}^{N=4} = \frac{\pi v}{3} (: I_R^A I_R^A : + : I_L^A I_L^A :) + \frac{v}{2} \left[(\partial_x \Phi)^2 + (\partial_x \Theta)^2 \right] + g \left[\cos(\sqrt{6\pi} \Phi) + \cos(\sqrt{6\pi} \Theta) \right] + 2\tilde{\lambda}_2 \text{Tr}(\Phi_{\text{adj}}) \cos(\sqrt{2\pi/3} \Phi), \quad (30)$$

with $g < 0$ and $\tilde{\lambda}_2 < 0$. The general structure of the field theory (30) leads us to expect that it is fully gapped in the \mathbb{Z}_4 and $\text{SU}(4)_2$ sectors. Indeed, we first note that the self-dual symmetry $\Phi \leftrightarrow \Theta$ is now explicitly broken due to the presence of the $\cos(\sqrt{2\pi/3} \Phi)$ term in Eq. (30). A mass gap for the \mathbb{Z}_4 degrees of freedom should be generated. Moreover, the $\text{SU}(4)_2$ perturbed by the relevant adjoint field is a massive field theory for either sign of its coupling constant and does not exhibit a massless flow as in the $\text{SU}(2n+1)_2$ case.^{68,70} We may conclude from these two facts that the two-leg $\text{SU}(4)$ zigzag spin ladder in the regime $J_1 \ll J_2$ is a fully gapped phase.

One can show the emergence of this gapped behavior by exploiting the fact that the UV-IR transmutation of some fields of the \mathbb{Z}_4 CFT along the massless RG flow (29) down to the \mathcal{M}_5 CFT has been obtained in Refs. 71 and 72. In particular, the leading contribution of the UV-IR transmutation of the operator $\cos(\sqrt{2\pi/3} \Phi)$ is:^{71,72}

$$\cos(\sqrt{2\pi/3} \Phi) \sim \sigma_{\mathbb{Z}_3} + \text{H.c.}, \quad (31)$$

where $\sigma_{\mathbb{Z}_3}$ is the \mathbb{Z}_3 spin field with scaling dimension $2/15$ of the \mathbb{Z}_3 CFT with central charge $c = 4/5$. In the far-IR limit, the low-energy physics which governs the properties of the two-leg $\text{SU}(4)$ zigzag spin ladder in the regime $J_1 \ll J_2$ is:

$$\mathcal{H}_{\text{zigzag}}^{N=4} = \frac{\pi v}{3} (: I_R^A I_R^A : + : I_L^A I_L^A :) + \mathcal{H}_{\mathbb{Z}_3} + 2\tilde{\lambda}_2 \text{Tr}(\Phi_{\text{adj}}) (\sigma_{\mathbb{Z}_3} + \text{H.c.}). \quad (32)$$

We use a simple mean-field analysis to investigate the IR properties of model (32). We decouple the $\text{SU}(4)_2$ and \mathbb{Z}_3 sectors to get the mean-field Hamiltonian density: $\mathcal{H}_{\text{mf}} = \mathcal{H}_1 + \mathcal{H}_2$ with:

$$\mathcal{H}_1 = \mathcal{H}_{\mathbb{Z}_3} + \kappa_1 (\sigma_{\mathbb{Z}_3} + \text{H.c.}) \quad (33)$$

$$\mathcal{H}_2 = \frac{\pi v}{3} (: I_R^A I_R^A : + : I_L^A I_L^A :) + \kappa_2 \text{Tr}(\Phi_{\text{adj}}),$$

with the mean-field coupling constants

$$\kappa_1 = 2\tilde{\lambda}_2 \langle \text{Tr}(\Phi_{\text{adj}}) \rangle$$

$$\kappa_2 = 2\tilde{\lambda}_2 \langle \sigma_{\mathbb{Z}_3} + \text{H.c.} \rangle. \quad (34)$$

The Hamiltonian \mathcal{H}_1 describes the scaling limit of the two-dimensional \mathbb{Z}_3 Potts model at $T = T_c$ in a magnetic field.⁷³ When $\kappa_1 < 0$, the magnetic field selects one specific color of the \mathbb{Z}_3 Potts model and the model is fully gapped. The Hamiltonian \mathcal{H}_2 of Eq. (33) describes an $\text{SU}(4)_2$ CFT perturbed by its adjoint primary field with scaling dimension $4/3$ which is a massive field theory for either sign of its coupling constant.⁷⁰ Since $\langle \sigma_{\mathbb{Z}_3} + \text{H.c.} \rangle > 0$ in the ground-state of \mathcal{H}_1 , we have $\kappa_2 < 0$ and a massive behavior occurs for \mathcal{H}_2 whose physical properties can be deduced from the identity:⁷⁴

$$\text{Tr}(\Phi_{\text{adj}}) = \text{Tr}(G^+ T^A G T^A)$$

$$\sim \text{Tr} G \text{Tr} G^+ - \frac{1}{4} \text{Tr}(G G^+), \quad (35)$$

where G is the WZNW $\text{SU}(4)$ matrix field. We thus find that the minimization of model \mathcal{H}_2 with $\kappa_2 < 0$ selects the center group of $\text{SU}(4)$:

$$G = \exp(i\pi k/2) I, \quad (36)$$

with $k = 0, 1, 2, 3$. From Eq. (17), we deduce that this solution breaks spontaneously T_{a_0} . The gapped phase is thus four-fold degenerate and the tetramerization phase of the weak-coupling limit $J_2 \ll J_1$ extends to the large J_2 regime in stark contrast to the odd- N case.

III. NUMERICAL CALCULATIONS

We have performed ED simulations on periodic chains using lattice symmetries as well as color conservation, which allows to reach $L = 27$ for $N = 3$ and $L = 24$ for $N = 4$ and to get the quantum numbers of the ground-state and its lowest excitations, hence suggesting possible symmetry breaking in the thermodynamic limit. In order to go beyond, we have used infinite-size DMRG (iDMRG) using the `ITensors.jl`⁷⁵ library and its subpackage `ITensorInfiniteMPS.jl` with a unit-cell of size $2N$. We used color conservation as well to accelerate the convergence. The maximal bond dimension χ which has been increased up to 8192. Energies are converged below 10^{-9} for all χ , and the entropies are converged below 10^{-6} , except for $\chi = 8192$ in the gapless phases or at large J_2 .

Note that for convenience and up to some irrelevant constants and redefinitions of the energy scales, we can rewrite the Hamiltonian (1) using permutation operators \hat{P}_{ij} which

swap the two states on sites i and j , due to the generalized Pauli identity.⁶⁰

$$2 \sum_A S_i^A S_j^A = \hat{P}_{ij} - \frac{1}{N}. \quad (37)$$

We used these permutation operators to implement the Hamiltonian and fix $J_1 = 1$.

A. SU(3) case

We start the SU(3) case by revisiting former numerical results obtained by Corboz *et al.*⁵⁰ Using ED (up to $L = 21$) and level spectroscopy analysis on one hand, and finite DMRG on the other hand, they concluded to an intermediate trimerized phase for $0.45 \lesssim J_2 \lesssim 3.5$. In Fig. 2, we plot the relevant low-energy excitations above the SU(3) singlet ground-state and their quantum numbers. In the expected critical phase (including the known integrable case for $J_2 = 0$), the lowest excitation is in the nontrivial adjoint representation and has a momentum $2\pi/3$ as expected (the finite-size gap is a finite-size effect). However, for intermediate J_2 , there are well-defined level crossings so that the lowest excitation is a two-fold degenerate (SU(3)) singlet at momentum $\pm 2\pi/3$, as expected for a singlet trimerized phase in the thermodynamic limit. In the inset of Fig. 2, we have attempted to extrapolate the critical values using finite-size scaling: the first one nicely converges to $J_2^{c,1} \approx 0.48$ while the other one has stronger finite-size effects so that we have less accuracy $J_2^{c,2} = 2.1(1)$. These values are in quantitative agreement with the previous results,⁵⁰ as $J_2^{c,2}$ is plagued by very strong finite-size effects. Note also that the first critical value has also been found in Ref. 52.

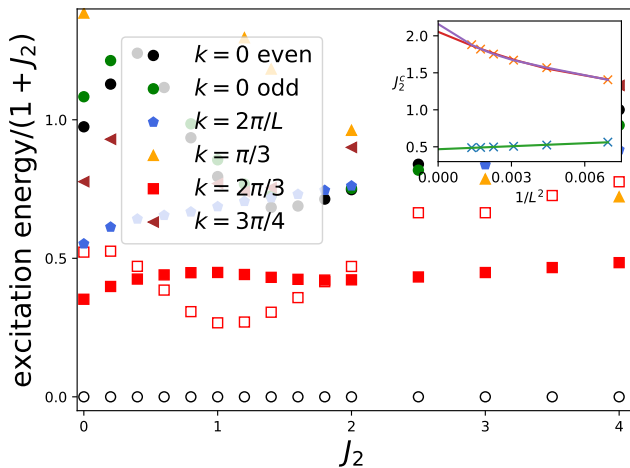


FIG. 2. Low-energy spectrum vs J_2 obtained by ED in the SU(3) case on the $L = 24$ periodic chain, for some relevant momenta. Open (respectively filled) symbols denote SU(3) singlet (respectively non-singlet) states. Inset: finite-size scaling of the level crossing between the lowest singlet or adjoint state at momentum $k = 2\pi/3$.

We have then performed iDMRG simulations with a compatible unit-cell of 6 sites for various bond dimensions χ . For intermediate J_2 , there is a very clear trimerized pattern in the bond amplitudes (see e.g. inset of Fig. 3) so that we define an order parameter as

$$T_{i,3} = \langle \hat{P}_{i,i+1} - \frac{1}{3} \sum_{k=0}^2 \hat{P}_{i+k,i+k+1} \rangle$$

which is measured in the ground-state obtained at fixed χ . Since the bond pattern can be shifted within our simulated unit cell, we choose to measure on bonds showing a weak/strong/strong pattern so that $T_{i,3}$ is positive and largest. Note that iDMRG technically breaks translation invariance, even after convergence, due to the initial edges. This effect, and the tendency to converge to less entangled superpositions allows us to directly use the trimerization as an order parameter, instead of a related correlation function. Data are shown in Fig. 3 and confirm that the trimerized singlet phase has a finite extent, in a range $0.5 \lesssim J_2 \lesssim 3.8$, larger than previously reported.⁵⁰ To resolve this disagreement, we performed a naive extrapolation in χ^{-1} of the trimerization using a second-degree polynomial fit to evaluate the infinite χ behavior. In the region $3.0 \lesssim J_2 \lesssim 4.0$, the trimerization strongly depends on χ . For too small bond dimensions, we do not resolve the gap and the matrix product states appear to belong to the large J_2 gapless phase, with a significant shift in the trimerization when varying χ . This crossover prevents us from reliably extrapolating any quantity for $J_2 \geq 3.4$. Because we observe this behavior at lower χ on well-converged system, we do not expect that we underestimate the extent of the gapped phase. The mismatch with the DMRG results of Ref. 50 is likely due to finite-size effects in the finite DMRG computation. This effect also prevents us to make a precise interpolation of the transition toward a gapless phase. Nevertheless, our numerical data do support a finite J_2 range for the trimerized phase.

The trimerization means that the SU(3) spins form singlets over three consecutive sites. This can be immediately seen by considering the entanglement spectrum and more precisely, the degeneracy of its largest eigenvalue. We define here the entanglement Hamiltonian at site n

$$H_{\text{ent}}(n) = -\log \text{Tr}_{s>n} |\Psi\rangle\langle\Psi|, \quad (38)$$

where s counts sites to the right of n , and we denote $\varepsilon_{\alpha,j}$ its j^{th} eigenvalue in the irrep α . This is readily accessible for matrix product states. In the gapless phase for $J_2 \leq 0.5$, the dominant eigenvalue is a singlet, with strict invariance by translation. Conversely, in the trimerized phase, the dominant eigenvalue form a repeating pattern of a singlet at site n , then a triplet (the fundamental or conjugate irrep) at site $n+1$ and $n+2$. This is the expected structure for a simple product state made of singlets on three consecutive sites. This pattern is a clear marker of the trimerized phase, and, as seen in Fig. 4, gives similar estimations for the phase boundaries. Remarkably, close to the peak of trimerization, the states are close to such a product state. At $J_2 = 1.2$ and $\chi = 8192$, for the singlet cut, the largest eigenvalue of the density matrix is about

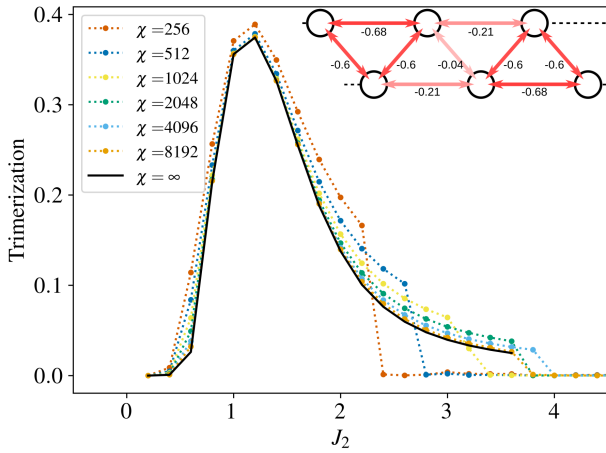


FIG. 3. Trimerization $T_{i,3}$ vs J_2 obtained by iDMRG in the SU(3) chain for various χ as well as its extrapolation to infinite bond dimension using a naive second degree polynomial fit in the regime $J_2 \leq 3.6$ where we can reliably perform this extrapolation. The trimerized phase (see the inset) opens up at $J_2 \approx 0.5$, and extends, for the χ we have access to, to $J_2 \approx 3.8$. Then, crossovers with χ , visible as kinks in the trimerization, prevent us to perform a reliable scaling. In inset, we represent the numerically obtained bond energies $\langle \hat{P}_{ij} \rangle$ on each link where \hat{P}_{ij} is defined in Eq. (37). The structure of the singlet is directly visible.

0.745 (singlet state). The next ones are two quasi-degenerate octuplets (i.e. adjoint irrep) of total weight ≈ 0.125 each.

To complement these observables, we also investigated the correlation length ξ (either induced from the finite χ in the gapless phases, or by the gap) obtained from the leading eigenvalues of the transfer matrix, see Fig. 5. For a given irrep α , we define the associated correlation length

$$\xi_\alpha = \frac{2N}{\log t_{\alpha,1}}, \quad (39)$$

where $t_{\alpha,1}$ is the first (nontrivial in the singlet case) eigenvalue of the transfer matrix. For all J_2 , the shortest correlation length appears to be in the adjoint irrep **8** and appears to be finite in the trimerized phase, see Fig. 6. Even at the peak of trimerization, its value is about 30 sites. In order to limit the finite χ effects, we attempted to extrapolate ξ using different gaps in the transfer matrix as scaling parameters.⁷⁶ In particular, we used the gap between the first and third **8** irreps in the eigenvalues

$$\delta = \frac{1}{2N} \log \left(\frac{t_{8,3}}{t_{8,1}} \right), \quad (40)$$

and the gap between the first irrep **10** and the first irrep **8**. Both approaches led to similar results, suggestive of a finite region for the trimerized phase when $0.5 \lesssim J_2 \lesssim 3.8$, but significant level crossings with χ prevented us from getting a good approximation for the second transition point.

To further characterize the critical phases at small and large J_2 , we have also computed the entanglement entropy S in or-

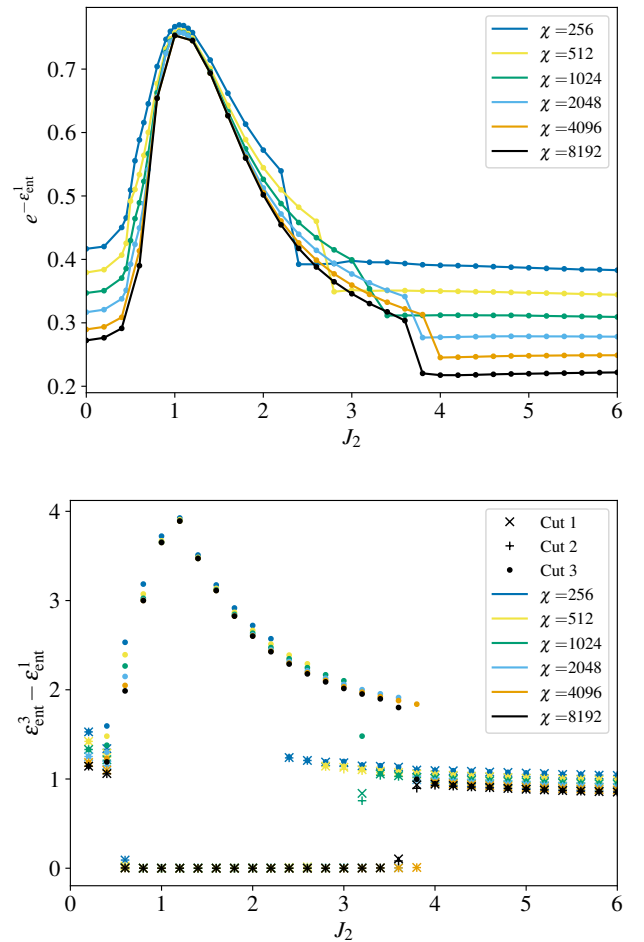


FIG. 4. Top: largest eigenvalue of the "mid-chain" reduced density matrix on the weakest bond of the unit-cell for the SU(3) chain, as defined in Eq. (38). The opening of the trimerized phase is characterized by a large peak where the matrix product state becomes close to a product state. At large J_2 , the discontinuity indicates when our simulations become unreliable. Bottom: gap between third and first entanglement energies. The singlet pattern 133 is characteristic of a product state of consecutive singlets. At large J_2 , the pattern becomes abruptly compatible with a gapless phase.

der to extract the central charge⁷⁷

$$S \sim \frac{c}{6} \ln \xi + b, \quad (41)$$

when fitting with respect to the correlation length ξ_8 or ξ_{10} . Data are shown in Fig. 7. For $J_2 < 0.5$, we obtain an excellent agreement with the expected value for $SU(3)_1$ criticality, namely $c = 2$, despite using a very naive fit with only c and b as parameters. In the intermediate trimerized phase, the entanglement entropy S saturates to a finite value. For large J_2 , we obtain large values of S , which necessarily limit the precision of our matrix product states. We measure an apparent effective $c \approx 3.2$, i.e. indicative of $SU(3)_2$ criticality⁷⁸. As discussed in Sec. II B 1, the low-energy approach starting from the zigzag regime, contains two different sectors, a first one

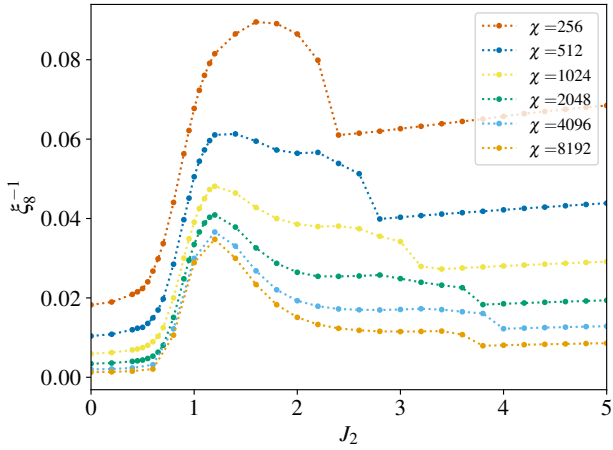


FIG. 5. Inverse correlation length ξ_8 vs J_2 obtained by iDMRG in the SU(3) chain for various χ . The gap opening at $J_2 \approx 0.5$ is immediately visible. The correlation length remains relatively large throughout the gapped phase. At large J_2 , we observe also kinks in the correlation length, which marks the crossover due to finite χ that spoils our analysis.

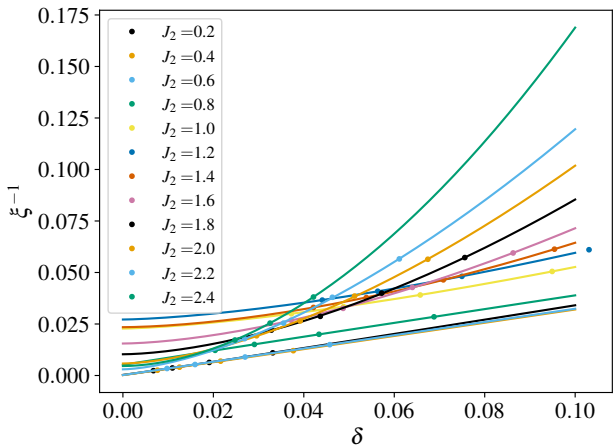


FIG. 6. Scaling of the inverse correlation length ξ vs δ obtained by iDMRG in the SU(3) case for various χ , see text.

described by Eq. (20) for the \mathbb{Z}_3 degrees of freedom which is fully gapped, and an $SU(3)_2$ one which enjoys a massless flow to $SU(3)_1$. The numerical observation of the $SU(3)_2$ criticality means that we resolve the \mathbb{Z}_3 gap but not the $SU(3)_1$ criticality with $c = 2$ obtained in the infrared regime. Related numerical problems were also noted in the context of the SU(3) Heisenberg spin chain in symmetric representation⁷⁹ and the correct quantum criticality has been obtained only by large-scale numerical simulations by exploiting the full non-Abelian SU(3) symmetry of the model.⁸⁰ Our numerical approach exploits the color conservation but does not take into account the full SU(3) symmetry. Hence, we expect that the observation of an apparent effective central charge $c \simeq 3.2$ is a crossover effect

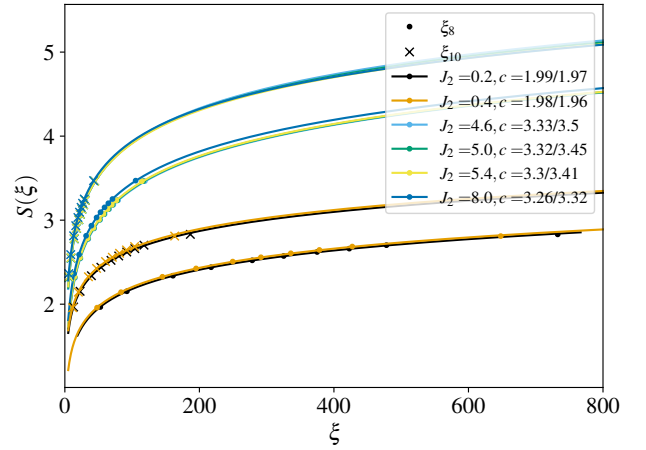


FIG. 7. Entanglement entropy vs correlation length obtained by iDMRG in the SU(3) chain for various χ , using the different correlation lengths we have access to. The lines are fit using the conformal formula in Eq. (41). At low J_2 , it matches the expected result of a $SU(3)_1$ critical theory. At large J_2 , it reliably indicates a $SU(3)_2$ CFT, probably due to finite χ , as discussed in the main text. The first indicated central charge is obtained using ξ_8 while the second one is obtained using ξ_{10} . They are in good agreement.

and c should tend to 2 for large enough ξ .

As a side note, we find the scaling with ξ_8 more practical than a scaling directly with χ : the effective exponents relating χ and ξ differ from Ref. 81. We find numerically that

$$\xi_8 = \chi^\kappa \quad (42)$$

with $\kappa \approx 0.7$ for $J_2 \leq 0.5$ and $\kappa \approx 0.60$ at large J_2 (to compare with 0.87 and 0.64 using the standard formula). Data can be found in Appendix D. This should not come as a surprise due to the large degeneracy of the entanglement spectrum enforced by the non-Abelian symmetry.

In the large J_2 limit for the SU(2) zigzag spin ladder, some incommensurability has been measured.³¹ This can be found using iDMRG by analyzing the imaginary part of the transfer matrix eigenvalues, see Appendix E. We define the incommensuration associated to the eigenvalue $t_{\alpha,j}$ of the transfer matrix by

$$\theta_{\alpha,j} = \frac{1}{2N} \text{Im} \log t_{\alpha,j}. \quad (43)$$

Strictly speaking, nonzero $\theta_{\alpha,j}$ means that we expect some correlations $\langle \hat{O}(x) \hat{O}(y) \rangle$ to oscillate as $\cos(2N\theta_{\alpha,j}(X - Y))$ where X (resp. Y) is the label of the unit-cell of x (resp. y). In practice, in our models, it is reasonable to expect that they will oscillate as $\cos((\theta_{\alpha,j} + \frac{2m\pi}{L})(x - y))$, with m an integer which cannot be determined directly from the transfer matrix. Our data for SU(3) shows no sign of finite incommensuration in the large χ limit, with nonzero θ remaining largely below 10^{-3} for eigenvalues of norm larger than 10^{-2} , i.e. purely finite convergence and finite χ effects.

B. SU(4) case

For the SU(4) case, we have performed extensive ED up to $L = 20$ ($L = 24$ for some parameters) periodic chains and the corresponding low-energy excitations are shown in Fig. 8. While the integrable $J_2 = 0$ case (corresponding to the critical Sutherland model) does exhibit a lowest excitation in the adjoint representation at momentum $\pm\pi/2$ as expected, we observe that for J_2 roughly larger than 1, the lowest excitation becomes a singlet with a π momentum difference from the ground-state, possibly indicating a singlet phase that breaks translation symmetry. Quite interestingly, these two lowest singlets are quasi degenerate for $J_2 \simeq 2$, although the model is quite simpler than the exact one showing a perfectly tetramerized VBS.⁸² For even larger J_2 , the first excitation still remains a singlet with a π momentum shift.

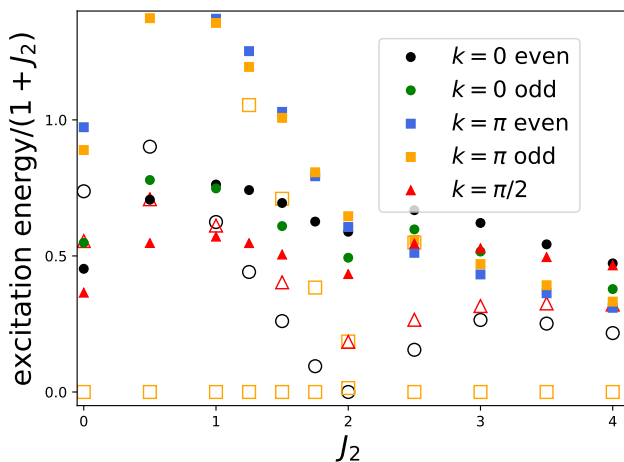


FIG. 8. Low-energy spectrum vs J_2 obtained by ED in the SU(4) case on $L = 20$ periodic chain. We have plotted only some particular momenta, relevant for the lowest excitations. Note that for $J_2 \geq 1$ the lowest excitation is a singlet with a momentum shift of π with respect to the groundstate.

In order to fully characterize this symmetry breaking, we have performed iDMRG simulations with a unit-cell of $2N = 8$ sites and various maximal bond dimensions χ . We define a tetramerization order parameter as

$$T_{i,4} = \langle \hat{P}_{i,i+1} - \frac{1}{4} \sum_{k=0}^3 \hat{P}_{i+k,i+k+1} \rangle$$

measured in the ground-state and choosing appropriate bonds so that it is positive and largest. Data are shown in Fig. 9 and are consistent with a critical value $J_2 \simeq 1$ for the transition between a critical phase and a tetramerized one which extends up to the large J_2 regime in agreement with the field theory prediction. Note that the apparent anomaly at $J_2 \simeq 4$ becomes less pronounced when increasing the bond dimension χ . We see no clear signs of the reopening of a uniform gapless phase at large J_2 , with significantly better stability and convergence than for SU(3). The J_2 bonds pattern exhibits

a $\pi/2$ modulation (strong/strong/strong/weak), see e.g. the corresponding modulation in inset of Fig. 9. As in the SU(3) case, this tetramerized phase appears to be adiabatically connected to the limit of a tensor product of singlets over four consecutive sites. The degeneracy of the largest eigenvalue of the entanglement spectrum, defined in Eq. (38), supports this picture, with a repeating pattern of **1** (trivial irrep), **4** (fundamental irrep), **6** (the fully antisymmetric self-conjugate irrep) and $\bar{\mathbf{4}}$ (the conjugate of the fundamental irrep). Similarly to the SU(3) limit, for $J_2 = 2.0$ and $\chi = 8192$, the largest eigenvalue of the reduced density matrix reaches about 0.811 in the singlet cut, while the second eigenvalue has a total weight of 0.104 in the irrep **15** (adjoint irrep), revealing how close the system is from the singlet product state.

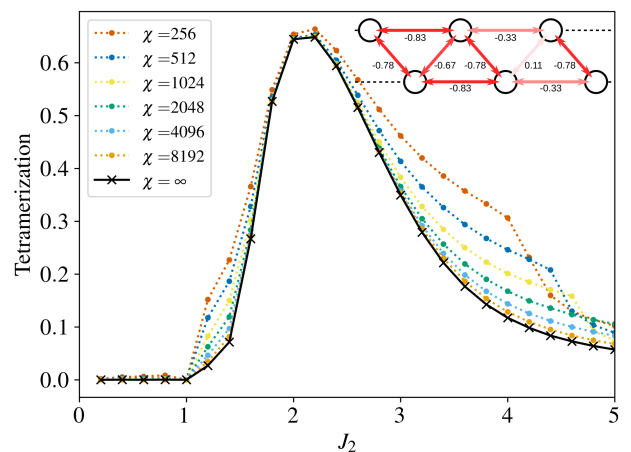


FIG. 9. Tetramerization $T_{i,4}$ vs J_2 obtained by iDMRG for the SU(4) chain for various χ as well as its extrapolation to infinite bond dimension using a naive second degree polynomial fit. The tetramerized phase opens at $J_2 \approx 1$, and remains nonzero up to the largest $J_2 = 8.0$ we considered. Small non-analyticities are nonetheless visible, revealing the finite χ and convergence problems at large J_2 . In inset, we represented the numerically obtained bond energies $\langle \hat{P}_{ij} \rangle$ for $J_2 = 2.0$, revealing the appearance of the singlet phase.

At large $J_2 \geq 5.0$, we see a crossover towards a degeneracy pattern of $(1, 2, 4, 2)$, which is also visible at lower J_2 and χ , and explain the small anomaly in the tetramerization for $J_2 \approx 5.0$, see Fig. 10. Note that this pattern is not SU(4) invariant, it is therefore a finite convergence and χ effect coming from the color conservation. Note that the gapless phase for $J_2 \leq 1$ is again characterized by a single, nondegenerate largest eigenvalue.

The dominant correlation length comes from the adjoint representation **15**, shown in Fig. 11, and is of the order of the unit-cell close to the maximum of tetramerization. We use as convergence parameters the gaps between the first and third adjoint irreps, and the gap $\xi_{10,1}^{-1} - \xi_{8,1}^{-1}$. Both leads to similar results for $J_2 \leq 4.5$, beyond which the finite χ effects are too large. The results are also coherent with a gapped phase remaining open for $J_2 \gg 1$.

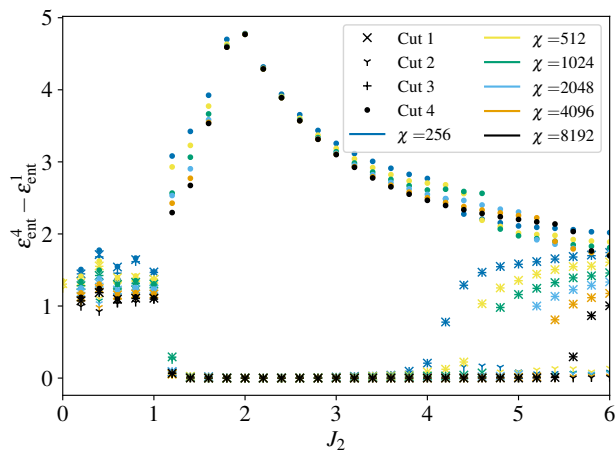
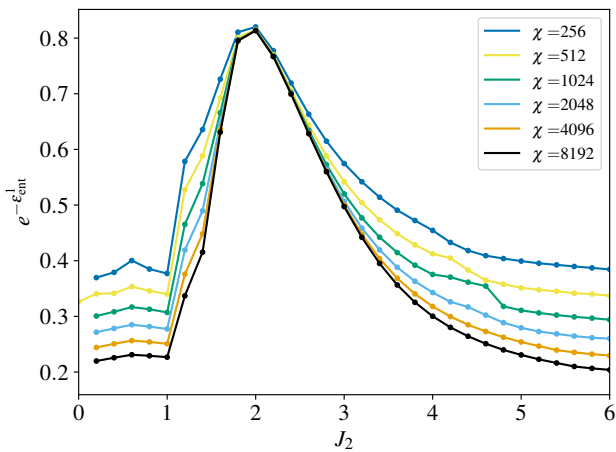


FIG. 10. Top: the largest eigenvalue of the "mid-chain" reduced density matrix on the weakest bond of the unit-cell for SU(4), as defined in Eq. (38). The opening of the tetramerized phase is characterized by a large peak where the matrix product state becomes close to a product state. Right: gap between sixth and first entanglement energies. The singlet pattern 1464 is characteristic of a product state of consecutive SU(4) singlets. We observe a breakdown of SU(4) at large J_2 due to finite χ .

We verified that the gapless phase for $J_2 \leq 1$ has central charge $c = 3$, using the scaling with the correlation lengths (see Fig. 12). We numerically found that $\xi_{15} \approx \chi^{0.6}$ instead of the naive $\chi^{2/3}$. For $J_2 > 5$, our bond dimension is too low to resolve the gap, despite the finite tetramerization. A naive fit of the entropy gives a central charge $c \approx 5.6$, only slightly reduced compared to two independent $c = 3$ chains. This estimate of the central charge seems to be consistent with the low-energy approach for $N = 4$ since, in the large J_2 regime, we expect a first crossover from the $c = 6$ decoupling regime to a critical regime with $c = 6 - (1 - 4/5) = 5.8$ which stems from the existence of the massless RG flow of model (29) from the \mathbb{Z}_4 $c = 1$ UV fixed point to the \mathbb{Z}_3 IR one with $c = 4/5$. In the far-IR regime, a fully gapped tetramerized phase should eventually emerge.

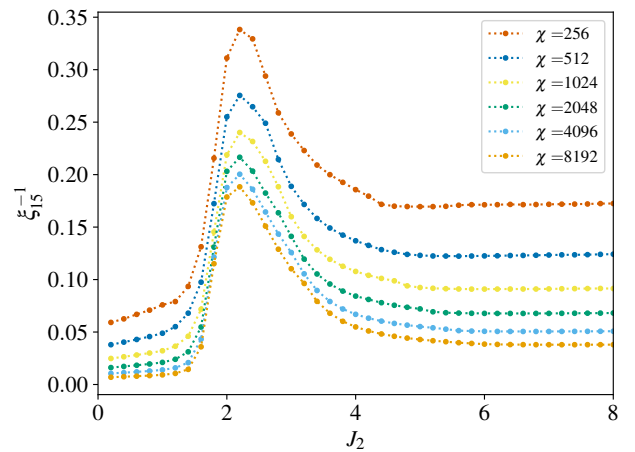


FIG. 11. Inverse correlation length ξ_{15}^{-1} vs J_2 obtained by iDMRG in the SU(4) chain for various χ . The gap opening at $J_2 \approx 0.5$ is immediately visible. The correlation length remains relatively large throughout the gapped phase. At large J_2 , we observe also kinks in the correlation length, which marks the crossover due to finite χ that spoil our analysis.

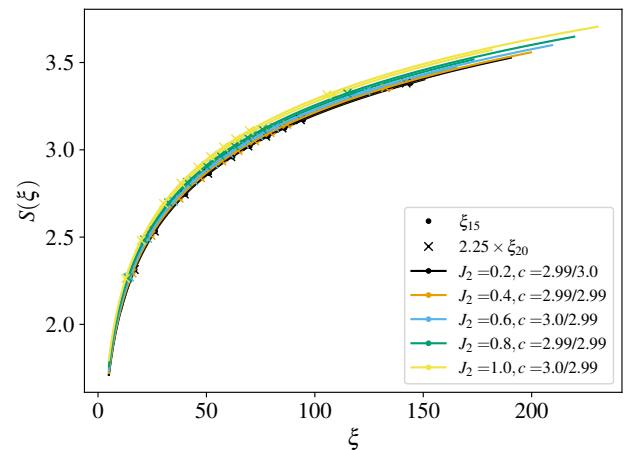
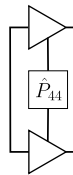


FIG. 12. Entanglement entropy vs correlation length obtained by iDMRG in the SU(4) chain for various χ for the different correlation lengths we used. The lines are fit using the conformal formula in Eq. (41). It matches the expected result of a SU(4)₁ critical theory for $J_2 \leq 1$. The first central charge is obtained using ξ_{15} while the second one is obtained with ξ_{20} .

Finally, a careful investigation of the transfer matrix revealed a commensurate-incommensurate crossover at $J_2 \approx 2$, similar to the one observed in the SU(2) $J_1 - J_2$ spin chain. This incommensuration is not visible in the first nontrivial eigenvalues of the transfer matrix, even taking into account the different irreps. This is actually also the case for SU(2) spin chains close to the Majumdar-Ghosh point (See Appendix E). Unlike SU(2) though, the incommensurate eigenvalues never become dominant in the regime where we reliably measure incommensuration (for $J_2 \leq 4.0$). As an example, for $J_2 = 2.2$

and $\chi = 8192$, the first non trivial values are $t_{15,1} \approx 0.221$ and we see incommensuration in this irrep only for a smaller eigenvalue $t_{15,j}^{inc} \approx -0.023 + 0.040i$. Note that for this J_2 and χ , the entropy is converged at 10^{-9} and the absolute value of $t_{15,j}^{inc}$ slowly increases with χ . At larger $J_2 = 4.0$ and $\chi = 8192$, we have $t_{15,1} \approx 0.645$ and the first incommensuration for $t_{15,4}^{inc} \approx 0.456 - 0.014i$. Therefore, given the clear converged signal shown in Fig. 13, we are confident that this incommensuration is not a numerical artifact. Within our precision, the commensurate-incommensurate crossover coincides with the point where the singlets are maximally localized, i.e., when the entropy between the 4th and 5th sites of the unit-cell is minimal. The natural interpretation of our data is that the incommensuration opens only in a specific excitation channel with a significantly larger gap. We verified that the corresponding right eigenvector has nonzero overlap with the tensor



where \hat{P}_{44} is the local projector on $(0, 0, 0, 1)$ and the triangles denote the left canonical matrix product state. Hence, the incommensuration will be observable in the spin-spin correlations in the form of some $\cos(\theta(x-y))$ modulations, although they are subdominant (see Appendix D).

It is tempting to explain the numerical evidence of this incommensuration for $N = 4$ by the existence of a nonzero conformal spin operator, a twist term, in the low-energy approach of the two-leg zigzag spin ladder (2). Such spin-1 conformal spin operator, $N_1^A \partial_x N_2^A$, with scaling dimension $3 - 2/N$ has been conjectured in Ref. 33 to be the source of the incommensuration of the $SU(2) J_1 - J_2$ Heisenberg spin chain. Such an operator is marginal in the $N = 2$ whereas slightly irrelevant when $N = 4$, a fact which is consistent with the subdominant incommensurate behavior observed for $N = 4$.

IV. CONCLUSION

Using complementary analytical and numerical techniques, we have investigated the ground-state phase diagram of the $J_1 - J_2$ $SU(N)$ antiferromagnetic Heisenberg spin chain, in the fundamental representation, which is a minimal model to study frustration effect in $SU(N)$ chains. By varying the sole parameter J_2/J_1 , we have shown that different phases can emerge. First, the well-known (integrable) case at $J_2 = 0$ corresponds to an $SU(N)_1$ critical phase (Luttinger liquid) with $c = N - 1$ gapless modes, which has a finite extension for all N . Then, for $J_2 > J_2^{c,1}$, the system enters an N -merized phase which breaks spontaneously lattice translation symmetry (also known as a valence bond solid or VBS) and which can be understood as being adiabatically connected to a product of $SU(N)$ singlets (made of N consecutive sites). Such a perfect $SU(N)$ VBS is the exact ground-state of parent Hamiltonians with multi-site interactions⁸² and fine tuned

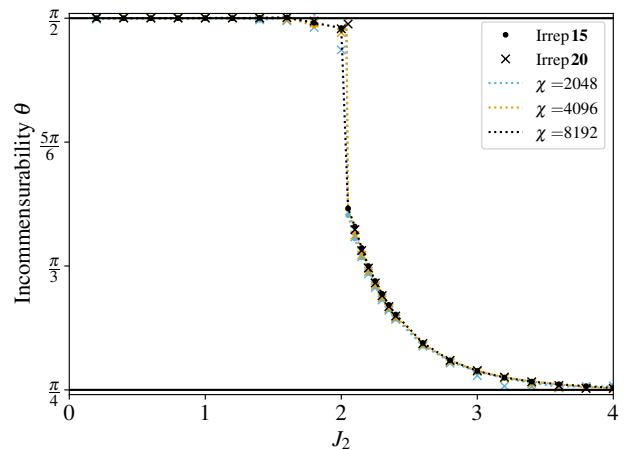


FIG. 13. Incommensuration measured as in Eq. (43) for the $SU(4)$ chain as a function of J_2 for various χ . Unlike the $SU(3)$ chain, incommensuration appears for $J_2 \approx 2.0$, close to the point with the shortest correlation length. The complex eigenvalues start one order of magnitude smaller than the dominant eigenvalues, and appear (at least) in the singlet and adjoint irrep. Note that with our choice of unit-cell, the incommensurability is only defined modulo $\pi/4$. We suggestively chose $\theta = \frac{\pi}{2}$ for $J_2 < 2$ as it matches the pattern induced by the four sites singlets in an open chain.

parameters, while our microscopic model appears to be more realistic. In the N -merized phase, the low-lying excitations are made of $SU(N)$ spinons with fractional quantum numbers which have been shown, within the low-energy approach, to belong to the \bar{N} irrep of the $SU(N)$ group. As in the $N = 2$ case, these spinons can be viewed as domain-wall configurations between the N -degenerate ground states of the N -merized phase.

For very strong J_2 , the nature of the ground-state crucially depends on the parity of N : for even N , there is no other phase transition and the chain remains in a gapped N -merized phase that breaks translation symmetry; conversely, for odd N , the N -merized phase has only a finite extension and gives rise to another $SU(N)_1$ gapless phase which persists for $J_2/J_1 \rightarrow \infty$. On top of this quantitative difference between even and odd N , we have numerically observed a much subtle effect with the emergence of an incommensurate behavior when $N = 4$. Our iDMRG simulations have revealed a nonzero imaginary part of some transfer matrix eigenvalues, leading to incommensurate spin-spin correlations for $N = 2, 4$ whereas no incommensuration is found for $N = 3$. The incommensurate behavior for $N = 4$ is reminiscent of the behavior found for $SU(2)$ in Ref. 31 with incommensurate correlations above the Majumdar-Ghosh point, the main difference being that the incommensuration is subdominant in the spin-spin correlation function for $SU(4)$.

As perspectives, it would be worth investigating the physical origin of this incommensuration phenomenon, as well as checking if it exists for all even N . From a numerical point of view, we have discussed the difficulty of simulating the regime $J_2 \gg J_1$, in particular to get the correct criticality

for $N = 3$ or to get an accurate second critical value, which could be overcome using full $SU(N)$ symmetry in the simulations.^{79,83} Finally, due to the experimental realizations of $SU(N)$ -symmetric interactions in ultracold atomic gases, it will be very interesting to investigate experimentally the competition, revealed here in a simple model, between magnetic ordering and valence-bond solids.

ACKNOWLEDGMENTS

We would like to thank Matt Fishman, Olivier Gauthé, Frédéric Mila, and Keisuke Totsuka for useful discussions. S. C. acknowledges the use of HPC resources from CALMIP (Grant No. 2022-P0677) and GENCI (Project No. A0110500225). L. H. has been supported by the Swiss National Science Foundation (FM) Grant No. 182179. Part of the simulations have been performed on the facilities of the Scientific IT and Application Support Center of EPFL. S.C. and P.L. would like to thank CNRS for constant support over the years and acknowledge the financial support (grant CNRS IRP EXQMS).

Appendix A: Abelian-bosonization description of the N -merized phase

In this Appendix, we use the Abelian-bosonization approach to model (1) in the weak-coupling limit $J_2 \ll J_1$ to describe the low-energy properties of the N -merized phase.

As is well-known, the physical properties of the $SU(N)$ Sutherland model, e.g. model (1) with $J_2 = 0$, can be obtained from the large repulsive U limit of the $U(N)$ Hubbard chain at $1/N$ -filling with Hamiltonian:^{36,37,56}

$$H_U = -t \sum_i \sum_{\alpha=1}^N \left(c_{\alpha,i+1}^\dagger c_{\alpha,i} + \text{H.c.} \right) + \frac{U}{2} \sum_{i,\alpha,\beta} n_{\alpha,i} n_{\beta,i} (1 - \delta_{\alpha\beta}), \quad (\text{A1})$$

where $c_{\alpha,i}^\dagger$ creates a fermion with color $\alpha = 1, \dots, N$ of the site i and $n_{\alpha,i} = c_{\alpha,i}^\dagger c_{\alpha,i}$ is the occupation number. When U is sufficiently large, the system becomes a Mott insulator and the charge degrees of freedom gets decoupled from the low-energy physics.^{37,39} The latter is described by the $SU(N)$ Sutherland model with an $SU(N)$ spin operator on site i which reads as follows in terms of the lattice fermions:

$$S_i^A = c_{\alpha,i}^\dagger T_{\alpha\beta}^A c_{\beta,i}, \quad (\text{A2})$$

where T^A are the generators of the N -representation of $SU(N)$ normalized such that $\text{Tr}(T^A T^B) = \delta^{AB}/2$. Using the continuum limit of the lattice fermion operators in terms of N left-right moving Dirac fermions: $c_{\alpha,i}/\sqrt{a_0} \rightarrow e^{-ik_F x} L_\alpha(x) + e^{ik_F x} R_\alpha(x)$ (with $k_F = \pi/(Na_0)$), one gets the low-energy identification as in Eq. (4):

$$S_i^A/a_0 \rightarrow J_R^A + J_L^A + e^{i2k_F x} N^A + \text{H.c.} + \dots, \quad (\text{A3})$$

where $J_L^A = L_\alpha^\dagger T_{\alpha\beta}^A L_\beta$ is the left $SU(N)_1$ current with a similar definition for the right one. In Eq. (A3), the $2k_F$ $SU(N)$ spin density is $N^A = \langle L_\alpha^\dagger T_{\alpha\beta}^A R_\beta \rangle_c$, the average being over the fully gapped charge mode. The Hamiltonian density (7) which captures the IR physical properties of the $J_1 - J_2$ $SU(N)$ Heisenberg spin chain in the weak-coupling $J_2 \ll J_1$ can be expressed in terms of the Dirac fermions:

$$\begin{aligned} \mathcal{H}_{J_1-J_2} &= \frac{2\pi v}{N+1} (: J_R^A J_R^A : + : J_L^A J_L^A :) + \lambda J_R^A J_L^A \\ &= -iv (: R_\alpha^\dagger \partial_x R_\alpha : - : L_\alpha^\dagger \partial_x L_\alpha :) + \frac{\lambda}{2} R_\alpha^\dagger R_\beta L_\beta^\dagger L_\alpha \\ &\quad - \frac{\lambda}{2N} : R_\alpha^\dagger R_\alpha : : L_\beta^\dagger L_\beta :, \end{aligned} \quad (\text{A4})$$

where we have used the identity:

$$T_{\alpha\beta}^A T_{\gamma\delta}^A = \frac{1}{2} \left(\delta_{\alpha\delta} \delta_{\beta\gamma} - \frac{1}{N} \delta_{\alpha\beta} \delta_{\delta\gamma} \right). \quad (\text{A5})$$

We introduce now N left-right moving bosons $\varphi_{\alpha L,R}$ to bosonize the Dirac fermions in Eq. (A4):^{56,59}

$$\begin{aligned} L_\alpha &= \frac{\kappa_\alpha}{\sqrt{2\pi a_0}} e^{-i\sqrt{4\pi}\varphi_{\alpha L}}, \\ R_\alpha &= \frac{\kappa_\alpha}{\sqrt{2\pi a_0}} e^{i\sqrt{4\pi}\varphi_{\alpha R}}, \end{aligned} \quad (\text{A6})$$

where $[\varphi_{\alpha R}, \varphi_{\beta L}] = i\delta_{\alpha\beta}/4$ and κ_α are Klein factors to ensure the anticommutation of fermions with different colors: $\{\kappa_\alpha, \kappa_\beta\} = 2\delta_{\alpha\beta}$, $\kappa_\alpha^\dagger = \kappa_\alpha$. The $2k_F$ $SU(N)$ spin density can thus be expressed in terms of these bosonic fields:

$$N^A = \frac{\kappa_\alpha \kappa_\beta i^{\delta_{\alpha\beta}}}{2\pi a_0} T_{\alpha\beta}^A \langle e^{i\sqrt{4\pi}\varphi_{\alpha L} + i\sqrt{4\pi}\varphi_{\beta R}} \rangle_c. \quad (\text{A7})$$

It is then helpful to introduce a new basis with one charge bosonic field $\Phi_{cR,L}$ and $N-1$ spin fields $\Phi_{smR,L}$ ($m = 1, \dots, N-1$) to perform the charge average:³⁹

$$\begin{aligned} \Phi_{cR,L} &= \frac{1}{\sqrt{N}} \sum_{\alpha=1}^N \varphi_{\alpha R,L} \\ \Phi_{smR,L} &= \frac{1}{\sqrt{m(m+1)}} \left(\sum_{p=1}^m \varphi_{pR,L} - m\varphi_{m+1R,L} \right), \end{aligned} \quad (\text{A8})$$

the inverse transformation being:

$$\begin{aligned} \varphi_{\alpha R,L} &= \frac{\Phi_{cR,L}}{\sqrt{N}} + \sum_{m=1}^{N-1} e^{im} \Phi_{smR,L} \\ &= \frac{\Phi_{cR,L}}{\sqrt{N}} + \vec{e}_\alpha \cdot \vec{\Phi}_{sR,L}, \end{aligned} \quad (\text{A9})$$

where \vec{e}_α ($\alpha = 1, \dots, N$) are $N-1$ -dimensional vectors which satisfy:

$$\sum_{\alpha=1}^N \vec{e}_\alpha = \vec{0}, \quad (\text{A10a})$$

$$\sum_{\alpha=1}^N [\vec{e}_\alpha]^m [\vec{e}_\alpha]^{m'} = \delta_{mm'}, \quad (\text{A10b})$$

$$\vec{e}_\alpha \cdot \vec{e}_\beta = \delta_{\alpha\beta} - \frac{1}{N}, \quad (\text{A10c})$$

where $m = 1, \dots, N-1$ describes the components of the \vec{e}_α vectors. An explicit choice is:

$$[\vec{e}_\alpha]^m = \begin{cases} \frac{1}{\sqrt{m(m+1)}} & (m \geq \alpha) \\ -\sqrt{\frac{m}{m+1}} & (m = \alpha - 1) \\ 0 & (m < \alpha - 1) \end{cases}. \quad (\text{A11})$$

A free-field representation of the $SU(N)_1$ WZNW g primary field can then be obtained using Eq. (A7) and the identity (5):

$$g_{\beta\alpha} = \frac{\kappa_\alpha \kappa_\beta i^{\delta_{\alpha\beta}-1}}{\sqrt{N}} : e^{i\sqrt{4\pi}\vec{e}_\alpha \cdot \vec{\Phi}_{sL} + i\sqrt{4\pi}\vec{e}_\beta \cdot \vec{\Phi}_{sR}} :. \quad (\text{A12})$$

A more rigorous free-field representation of the g WZNW field can be found in Ref. 84 (see Appendix B) where the Klein factors are constructed out of the zero mode operators of the spin bosonic fields. From the correspondence (A12), we deduce an Abelian bosonization of the N -merization operator (8):

$$e^{-i\frac{2\pi n}{N}} S_n^A S_{n+1}^A \sim \text{Tr}g = \frac{1}{\sqrt{N}} \sum_{\alpha=1}^N e^{i\sqrt{4\pi}\vec{e}_\alpha \cdot \vec{\Phi}_s}, \quad (\text{A13})$$

where $\vec{\Phi}_s = \vec{\Phi}_{sL} + \vec{\Phi}_{sR}$. Since the WZNW g field is the elementary primary field of the $SU(N)_1$ CFT, the bosonic field $\vec{\Phi}_s$ is compactified with the following redundancy which leaves invariant (A13):

$$\vec{\Phi}_s \sim \vec{\Phi}_s + \sqrt{\pi} \sum_{i=1}^{N-1} n_i \vec{\alpha}_i, \quad (\text{A14})$$

n_i being integers. In Eq. (A14), $\vec{\alpha}_i$ ($i = 1, \dots, N-1$) are the simple roots ($\vec{\alpha}_i = \vec{e}_i - \vec{e}_{i+1}$) which generate the root lattice Q of the Lie algebra of $SU(N)$.

Model (A4) can then be bosonized using Eqs. (A6, A9):

$$\begin{aligned} \mathcal{H}_{J_1-J_2} = & v \left(\left(\partial_x \vec{\Phi}_{sR} \right)^2 + \left(\partial_x \vec{\Phi}_{sL} \right)^2 \right) + \frac{\lambda}{2\pi} \partial_x \vec{\Phi}_{sR} \cdot \partial_x \vec{\Phi}_{sL} \\ & - \frac{\lambda}{4\pi^2 a_0^2} \sum_{1 \leq \alpha < \beta \leq N} \cos \left(\sqrt{4\pi} (\vec{e}_\alpha - \vec{e}_\beta) \cdot \vec{\Phi}_s \right). \end{aligned} \quad (\text{A15})$$

A similar expression has been obtained before in the bosonization approach of the $U(N)$ Thirring model⁸⁵ whose low-energy properties are governed by model (A4). We introduce the set of positive roots Δ_+ of the Lie algebra of $SU(N)$:

$$\Delta_+ = \{ \vec{e}_\alpha - \vec{e}_\beta \mid 1 \leq \alpha < \beta \leq N \}, \quad (\text{A16})$$

to get:

$$\begin{aligned} \mathcal{H}_{J_1-J_2} = & v \left(\left(\partial_x \vec{\Phi}_{sR} \right)^2 + \left(\partial_x \vec{\Phi}_{sL} \right)^2 \right) + \frac{\lambda}{2\pi} \partial_x \vec{\Phi}_{sR} \cdot \partial_x \vec{\Phi}_{sL} \\ & - \frac{\lambda}{4\pi^2 a_0^2} \sum_{\vec{\alpha} \in \Delta_+} \cos \left(\sqrt{4\pi} \vec{\alpha} \cdot \vec{\Phi}_s \right). \end{aligned} \quad (\text{A17})$$

When $\lambda > 0$, the interacting part of model (A4) is a marginal relevant operator and a perturbative spectral gap is

formed. Its bosonized description (A17) takes the form of a sum of sine-Gordon models. In the fully gapped phase, the bosonic fields $\vec{\Phi}_s$ are pinned in the degenerate minima of the cosine potential of Eq. (A17):

$$\langle \vec{\Phi}_s \rangle = \sqrt{\pi} \sum_{i=1}^{N-1} p_i \vec{\omega}_i, \quad (\text{A18})$$

p_i being integers. In Eq. (A18), $\vec{\omega}_i$ ($i = 1, \dots, N-1$) are the fundamental weights which generate the weight lattice P of the Lie algebra of $SU(N)$. They are defined as follows in terms of the \vec{e}_α vectors (A10):

$$\vec{\omega}_i = \sum_{j=1}^i \vec{e}_j, \quad (\text{A19})$$

so that $\vec{\omega}_i \cdot \vec{\alpha}_j = \delta_{ij}$. Using the identification (A14), we find that the ground state of model (A17) is N -fold degenerate since the ratio P/Q of the $SU(N)$ lattices is isomorphic to the center of $SU(N)$: $P/Q \sim \mathbb{Z}_N$.⁶⁴ The N inequivalent ground states $|k\rangle$, $k = 0, \dots, N-1$ of the sine-Gordon models (A17) are chosen such that:

$$\langle \vec{\Phi}_s \rangle = -\sqrt{\pi} \vec{\omega}_k, \quad (\text{A20})$$

with the convention $\vec{\omega}_0 = \vec{0}$. In these ground states, the N -merization operator (A13) takes N different values since

$$\langle \text{Tr}g \rangle = \sqrt{N} e^{i\frac{2k\pi}{N}}. \quad (\text{A21})$$

This signals the spontaneous breaking of the one-step translation symmetry T_{a_0} in the N -merized phase since under T_{a_0} the $SU(N)_1$ WZNW g field transforms as $g \rightarrow e^{i\frac{2\pi}{N}} g$ (see Eq. (9)).

The low-lying excitations of the N -merized phase are massive solitons and anti-solitons of the sine-Gordon models (A17) which represent domain walls between different ground states $|k\rangle$ and $|k+1\rangle$, ($k = 0, \dots, N-1$) of the N -merized phase (with the identification $|N\rangle = |0\rangle$). From Eq. (A20), we deduce that the field configurations related to such solitons are

$$\vec{\Phi}_s(\infty) - \vec{\Phi}_s(-\infty) = -\sqrt{\pi} (\vec{\omega}_{k+1} - \vec{\omega}_k), \quad (\text{A22})$$

with the identification $\vec{\omega}_N = \vec{\omega}_0 = \vec{0}$. The quantum numbers of these excitations can be determined by considering the $N-1$ mutual commuting conserved charges Q^m ($m = 1, \dots, N-1$) of model (A4). They correspond to the $N-1$ diagonal Cartan generators H^m in the defining representation N :

$$[H^m]_{\alpha\beta} = \frac{1}{\sqrt{2m(m+1)}} \delta_{\alpha\beta} \left(\sum_{l=1}^m \delta_{\beta l} - m \delta_{\beta, m+1} \right). \quad (\text{A23})$$

Using Eqs. (A2, A3) and the bosonized descriptions (A6, A8), the Q^m charges are given by:

$$\vec{Q} = \frac{1}{\sqrt{2\pi}} \int_{-\infty}^{\infty} dx \partial_x \vec{\Phi}_s. \quad (\text{A24})$$

We deduce that the quantum numbers \vec{Q}_{k+1} of the excitation (A22) between the two consecutive ground states $|k\rangle$ and $|k+1\rangle$ ($k = 0, \dots, N-1$) are

$$\vec{Q}_{k+1} = -\frac{\vec{\omega}_{k+1} - \vec{\omega}_k}{\sqrt{2}} = -\frac{\vec{e}_{k+1}}{\sqrt{2}}. \quad (\text{A25})$$

From Eq. (A11), we observe that the N quantum numbers (A25) correspond to the N weight vectors of the conjugate \bar{N} -representation of the $SU(N)$ group which are the opposite of the weights of the N -representation. For instance, in the $N = 3$ case, we have from Eqs. (A25, A11):

$$\begin{aligned} \vec{Q}_1 &= -\left(\frac{1}{2}, \frac{1}{2\sqrt{3}}\right), \quad \vec{Q}_2 = -\left(-\frac{1}{2}, \frac{1}{2\sqrt{3}}\right), \\ \vec{Q}_3 &= \left(0, \frac{1}{\sqrt{3}}\right), \end{aligned} \quad (\text{A26})$$

and in the $N = 4$ case, we have:

$$\begin{aligned} \vec{Q}_1 &= -\left(\frac{1}{2}, \frac{1}{2\sqrt{3}}, \frac{1}{2\sqrt{6}}\right), \quad \vec{Q}_2 = -\left(-\frac{1}{2}, \frac{1}{2\sqrt{3}}, \frac{1}{2\sqrt{6}}\right), \\ \vec{Q}_3 &= -\left(0, -\frac{1}{\sqrt{3}}, \frac{1}{2\sqrt{6}}\right), \quad \vec{Q}_4 = \left(0, 0, \frac{1}{2}\sqrt{\frac{3}{2}}\right). \end{aligned} \quad (\text{A27})$$

The massive solitons of the N -merized phase share thus the same quantum numbers as the original gapless spinons of the Sutherland model which transform in the \bar{N} -representation of $SU(N)$.^{47,48} The latter become massive in the N -merized phase but still deconfined excitations that correspond to the domain-wall excitations between the N -degenerate ground states. Similarly, the anti-kinks of the N -merized phase transform in the N -representation of $SU(N)$ and can be viewed as massive $SU(N)$ anti-spinons.

Appendix B: Identification of fields

In this Appendix, we exploit the conformal embedding (15) to rewrite the interacting part of the Hamiltonian density (13) in terms of the fields in the $SU(N)_2 \times \mathbb{Z}_N$ basis. We use a different approach than the one presented in Ref. 58.

We introduce two operators written in terms of the WZNW fields of the $SU(N)_1 \times SU(N)_1$ CFT

$$\begin{aligned} \mathcal{O}_1 &= \text{Tr}(g_1 g_2^\dagger) \\ \mathcal{O}_2 &= \text{Tr}g_1 \text{Tr}g_2^\dagger - \frac{1}{N} \text{Tr}(g_1 g_2^\dagger). \end{aligned} \quad (\text{B1})$$

In this Appendix, we find the expression of these fields in the $SU(N)_2 \times \mathbb{Z}_N$ basis. In particular, we show that \mathcal{O}_1 does not depend on the $SU(N)_2$ degrees of freedom and is a primary field of the \mathbb{Z}_N CFT with conformal weights $h, \bar{h} = (N-1)/N$:

$$\begin{aligned} T_{\mathbb{Z}_N}(z)\mathcal{O}_1(0,0) &\sim \frac{N-1}{Nz^2}\mathcal{O}_1(0,0) + \frac{1}{z}\partial\mathcal{O}_1(0,0) \\ T_{SU(N)_2}(z)\mathcal{O}_1(0,0) &\sim 0, \end{aligned} \quad (\text{B2})$$

where $T_{\mathbb{Z}_N}$ (respectively $T_{SU(N)_2}$) is the stress-energy tensor of the \mathbb{Z}_N (respectively $SU(N)_2$) CFT. We have similar equations for the antiholomorphic sector that we will not consider

here for simplicity. It is also shown that the operator \mathcal{O}_2 is a primary field of the $\mathbb{Z}_N \times SU(N)_2$ CFT:

$$\begin{aligned} (T_{\mathbb{Z}_N} + T_{SU(N)_2})(z)\mathcal{O}_2(0,0) &\sim \frac{N-1}{Nz^2}\mathcal{O}_2(0,0) \\ &+ \frac{1}{z}\partial\mathcal{O}_2(0,0), \end{aligned} \quad (\text{B3})$$

with holomorphic weight $h = h_{\sigma_2} + h_{\text{adj}} = (N-2)/2N(N+2) + N/(N+2) = (N-1)/N$, h_{σ_2} (respectively h_{adj}) being the holomorphic weight of the \mathbb{Z}_N (respectively $SU(N)_2$) primary field σ_2 (respectively Φ_{adj}).

1. Preliminaries

We first present our normalization for the $SU(N)_1$ current which is defined by the following operator product expansion (OPE):

$$J_L^A(z)J_L^B(0) \sim \frac{\delta^{AB}}{8\pi^2 z^2} + \frac{if^{ABC}J_L^C(0)}{2\pi z}, \quad (\text{B4})$$

where f^{ABC} is the structure constants of the $SU(N)$ Lie algebra: $[T^A, T^B] = if^{ABC}T^C$. The stress-energy tensor of the $SU(N)_1$ CFT in our normalization is:

$$T_{SU(N)_1} = \frac{4\pi^2}{N+1} : J_L^A J_L^A :. \quad (\text{B5})$$

The defining OPE of the $SU(N)_1$ WZNW g field reads as:⁶⁴

$$\begin{aligned} J_L^A(z)g_{\alpha\beta}(0,0) &\sim -\frac{1}{2\pi z} T_{\alpha\gamma}^A g_{\gamma\beta}(0,0) \\ J_L^A(z)g_{\beta\alpha}^\dagger(0,0) &\sim \frac{1}{2\pi z} g_{\beta\gamma}^\dagger(0,0)T_{\gamma\alpha}^A, \end{aligned} \quad (\text{B6})$$

T^A being the generator which transforms in the fundamental representation of the $SU(N)$ group. Actually, we need the subleading contribution of the OPE (B6) to establish the relations (B2, B3). In this respect, let us now show that for an $SU(N)_1$ CFT, we have:

$$\begin{aligned} J_L^A(z)g_{\alpha\beta}(0,0) &\sim -\frac{1}{2\pi z} T_{\alpha\gamma}^A g_{\gamma\beta}(0,0) \\ &+ \frac{C}{2\pi} T_{\alpha\gamma}^A \partial g_{\gamma\beta}(0,0) \end{aligned} \quad (\text{B7})$$

$$\begin{aligned} J_L^A(z)g_{\beta\alpha}^\dagger(0,0) &\sim \frac{1}{2\pi z} g_{\beta\gamma}^\dagger(0,0)T_{\gamma\alpha}^A \\ &- \frac{C}{2\pi} \partial g_{\beta\gamma}^\dagger(0,0)T_{\gamma\alpha}^A, \end{aligned} \quad (\text{B8})$$

with $C = -N/(N-1)$.

Indeed, from Eq. (B7), we get:

$$\begin{aligned} g_{\alpha\beta}(x, \bar{w})J_L^A(w) &\sim -\frac{1}{2\pi(w-x)} T_{\alpha\gamma}^A g_{\gamma\beta}(x, \bar{w}) \\ &+ \frac{C}{2\pi} T_{\alpha\gamma}^A \partial g_{\gamma\beta}(w, \bar{w}) \\ &\sim \frac{1}{2\pi(x-w)} T_{\alpha\gamma}^A g_{\gamma\beta}(w, \bar{w}) \\ &+ \frac{(C+1)}{2\pi} T_{\alpha\gamma}^A \partial g_{\gamma\beta}(w, \bar{w}). \end{aligned} \quad (\text{B9})$$

We then consider the following OPE:

$$\begin{aligned} \overline{g_{\alpha\beta}(z, \bar{w})} : J_L^A J_L^A : (w) &= \frac{1}{2\pi i} \oint_w \frac{dx}{x-w} \left[\overline{g_{\alpha\beta}(z, \bar{w})} J_L^A(x) \right. \\ &\times \left. J_L^A(w) + J_L^A(x) \overline{g_{\alpha\beta}(z, \bar{w})} J_L^A(w) \right] \\ &= \frac{1}{2\pi i} \oint_w \frac{dx}{x-w} \left[\frac{1}{2\pi(z-x)} T_{\alpha\gamma}^A g_{\gamma\beta}(x, \bar{w}) J_L^A(w) \right. \\ &\left. + \frac{1}{2\pi(z-w)} J_L^A(x) T_{\alpha\gamma}^A g_{\gamma\beta}(w, \bar{w}) \right]. \end{aligned} \quad (\text{B10})$$

By using the results (B7, B9), we deduce:

$$\begin{aligned} g_{\alpha\beta}(z, \bar{w}) : J_L^A J_L^A : (w) &\sim \frac{N^2 - 1}{8\pi^2 N(z-w)^2} g_{\alpha\beta}(w, \bar{w}) \\ &+ \frac{N^2 - 1}{4\pi^2 N} \frac{C + 1/2}{z-w} \partial g_{\alpha\beta}(w, \bar{w}), \end{aligned} \quad (\text{B11})$$

and thus using the definition (B5)

$$\begin{aligned} g_{\alpha\beta}(z, \bar{w}) T_{SU(N)_1}(w) &\sim \frac{N-1}{2N(z-w)^2} g_{\alpha\beta}(w, \bar{w}) \\ &+ \frac{N-1}{N} \frac{C + 1/2}{z-w} \partial g_{\alpha\beta}(w, \bar{w}). \end{aligned} \quad (\text{B12})$$

Finally, we find

$$\begin{aligned} T_{SU(N)_1}(z) g_{\alpha\beta}(w, \bar{w}) &\sim \frac{N-1}{2N(z-w)^2} g_{\alpha\beta}(w, \bar{w}) \\ &- \frac{N-1}{N} \frac{C}{z-w} \partial g_{\alpha\beta}(w, \bar{w}). \end{aligned} \quad (\text{B13})$$

Since $g_{\alpha\beta}$ is an $SU(N)_1$ primary field with holomorphic weight $h = (N-1)/2N$, we have by definition

$$\begin{aligned} T_{SU(N)_1}(z) g_{\alpha\beta}(w, \bar{w}) &\sim \frac{N-1}{2N(z-w)^2} g_{\alpha\beta}(w, \bar{w}) \\ &+ \frac{\partial g_{\alpha\beta}(w, \bar{w})}{z-w}, \end{aligned} \quad (\text{B14})$$

and we thus obtain $C = -N/(N-1)$.

2. Identifications of $\mathcal{O}_{1,2}$ operators

We are now in position to show the identities (B2, B3). The holomorphic stress-energy tensors of two decoupled $SU(N)_1$ CFTs read as follows in terms of their currents:

$$\begin{aligned} T_{SU(N)_1 \times SU(N)_1} &= T_{SU(N)_1} + T_{SU(N)_1} \\ &= \frac{4\pi^2}{N+1} \sum_{l=1}^2 : J_{lL}^A J_{lL}^A :, \end{aligned} \quad (\text{B15})$$

while the $SU(N)_2$ one is in terms of the diagonal current $I_L^A = J_{1L}^A + J_{2L}^A$:

$$T_{SU(N)_2} = \frac{4\pi^2}{N+2} : I_L^A I_L^A :. \quad (\text{B16})$$

From the coset construction of the embedding (15), we deduce the stress-energy tensor of the \mathbb{Z}_N parafermionic CFT:

$$\begin{aligned} T_{\mathbb{Z}_N} &= \frac{4\pi^2}{(N+1)(N+2)} \left(\sum_{l=1}^2 : J_{lL}^A J_{lL}^A : \right. \\ &\left. - 2(N+1) J_{1L}^A J_{2L}^A \right). \end{aligned} \quad (\text{B17})$$

Using the fact that g_1 and g_2^\dagger are $SU(N)_1$ primaries field with holomorphic weight $h = (N-1)/2N$, we have

$$\begin{aligned} 4\pi^2 \sum_{l=1}^2 : J_{lL}^A J_{lL}^A : (z) \mathcal{O}_{1,2}(0,0) &\sim \frac{N^2 - 1}{Nz^2} \mathcal{O}_{1,2}(0,0) \\ &+ \frac{N+1}{z} \partial \mathcal{O}_{1,2}(0,0). \end{aligned} \quad (\text{B18})$$

We need also the following OPEs which can be deduced from the results (B7, B8):

$$\begin{aligned} 4\pi^2 J_{1L}^A J_{2L}^A : (z) \mathcal{O}_1(0,0) &\sim -\frac{N^2 - 1}{2Nz^2} \mathcal{O}_1(0,0) \\ &- \frac{N+1}{2z} \partial \mathcal{O}_1(0,0) \\ 4\pi^2 J_{1L}^A J_{2L}^A : (z) \mathcal{O}_2(0,0) &\sim \frac{1}{2Nz^2} \mathcal{O}_2(0,0) \\ &+ \frac{1}{2(N-1)z} \partial \mathcal{O}_2(0,0). \end{aligned} \quad (\text{B19})$$

It is now straightforward to check that the \mathcal{O}_1 field satisfies the OPEs (B2) which means that it is a singlet under the $SU(N)_2$ CFT and a \mathbb{Z}_N primary field with conformal weights $((N-1)/N, (N-1)/N)$ as $\Psi_{1L} \Psi_{1R}$:

$$\mathcal{O}_1 = \text{Tr}(g_1 g_2^\dagger) \sim \Psi_{1L} \Psi_{1R}. \quad (\text{B20})$$

Finally, we find that the \mathcal{O}_2 field satisfies the following OPEs from Eqs. (B18, B19):

$$\begin{aligned} T_{\mathbb{Z}_N}(z) \mathcal{O}_2(0,0) &\sim \frac{N-2}{N(N+2)z^2} \mathcal{O}_2(0,0) \\ &+ \frac{N-2}{(N-1)(N+2)z} \partial \mathcal{O}_2(0,0) \\ T_{SU(N)_2}(z) \mathcal{O}_2(0,0) &\sim \frac{N}{(N+2)z^2} \mathcal{O}_2(0,0) \\ &+ \frac{N^2}{(N-1)(N+2)z} \partial \mathcal{O}_2(0,0). \end{aligned} \quad (\text{B21})$$

We thus deduce that the \mathcal{O}_2 field satisfies the OPE (B3). It is not a singlet of \mathbb{Z}_N or $SU(N)_2$ CFTs but a primary field of the $\mathbb{Z}_N \times SU(N)_2$ CFT with holomorphic weight $h = h_{\sigma_2} + h_{\text{adj}} = (N-2)/N(N+2) + N/(N+2) = (N-1)/N$. One then obtains the correspondence:

$$\mathcal{O}_2 = \text{Tr} g_1 \text{Tr} g_2^\dagger - \frac{1}{N} \text{Tr}(g_1 g_2^\dagger) \sim \sigma_2 \text{Tr} \Phi_{\text{adj}}. \quad (\text{B22})$$

3. Sign ambiguity

The precise value of the coefficient in the identification (B20) is not important but its sign turns out to be crucial for the determination of the ground state of the two-leg $SU(N)$ zigzag ladder (2) in the limit $J_1 \ll J_2$. The approach, presented here, cannot fix the sign. We give here an additional argument that

$$\text{Tr}(g_1 g_2^\dagger) = a \Psi_{1L} \Psi_{1R}, \quad (\text{B23})$$

where a is necessarily positive.

In this respect, let us consider the following action which couples two $SU(N)_1$ CFTs:

$$\begin{aligned} \mathcal{S} &= \mathcal{S}[SU(N)_1; g_1] + \mathcal{S}[SU(N)_1; g_2] \\ &\quad - \int d^2x \left[\text{Tr}(g_1 g_2^\dagger) + \text{H.c.} \right], \end{aligned} \quad (\text{B24})$$

where the action of the $SU(N)_k$ WZNW model is given by:^{74,86}

$$\begin{aligned} \mathcal{S}[SU(N)_k; g] &= \frac{k}{8\pi} \int d^2x \text{Tr}(\partial^\mu g^\dagger \partial_\mu g) + \Gamma(g) \\ \Gamma(g) &= \frac{ik}{12\pi} \int_B d^3y \epsilon^{\alpha\beta\gamma} \text{Tr}(g^+ \partial_\alpha g g^+ \partial_\beta g g^+ \partial_\gamma g), \end{aligned} \quad (\text{B25})$$

g being an $SU(N)$ matrix field and $\Gamma(g)$ is the WZNW topological term. Using the conformal embedding (15) and the identification (B23), we get

$$\begin{aligned} \mathcal{S} &= \mathcal{S}[SU(N)_2; g] + \mathcal{S}_{\mathbb{Z}_N} \\ &\quad - a \int d^2x \left[\Psi_{1L} \Psi_{1R} + \text{H.c.} \right]. \end{aligned} \quad (\text{B26})$$

The interacting part acts only in the \mathbb{Z}_N sector and takes the form of the integrable perturbation (22) of the \mathbb{Z}_N parafermions. As discussed in the main text, a perturbative mass opens when a is positive and the action (B24) displays critical properties in the $SU(N)_2$ universality class with central charge $c = 2(N^2 - 1)/(N + 2)$. If $a < 0$, the \mathbb{Z}_N parafermions exhibit a massless RG flow and action (B24) has a central charge larger than $c = 2(N^2 - 1)/(N + 2)$.

We focus now directly on action (B24) and introduce the matrix $G = g_1 g_2^\dagger$ which is still an $SU(N)$ matrix. Using the Polyakov-Wiegmann formula:⁸⁷

$$\begin{aligned} \mathcal{S}[SU(N)_1; g_1] &= \mathcal{S}[SU(N)_1; G g_2] = \mathcal{S}[SU(N)_1; G] \\ &\quad + \mathcal{S}[SU(N)_1; g_2] - \frac{1}{4\pi} \int d^2x \text{Tr}(g_2^+ \partial g_2 G \bar{G} G^+), \end{aligned} \quad (\text{B27})$$

action (B24) simplifies as

$$\begin{aligned} \mathcal{S} &= \mathcal{S}[SU(N)_1; G] + 2\mathcal{S}[SU(N)_1; g_2] - \int d^2x \text{Tr}(G) + \text{H.c.} \\ &\quad - \frac{1}{4\pi} \int d^2x \text{Tr}(g_2^+ \partial g_2 G \bar{G} G^+). \end{aligned} \quad (\text{B28})$$

In the far-IR limit, the G field is pinned to the configuration $G = I$ and the fluctuations are massive. Integrating out these degrees of freedom, we get in the low-energy regime:

$$\mathcal{S} = 2\mathcal{S}[SU(N)_1; g_2] = \mathcal{S}[SU(N)_2; g_2], \quad (\text{B29})$$

and thus an $SU(N)_2$ critical behavior as it should be. This gives a strong argument that the identification (B23) with $a > 0$ is correct.

Appendix C: Semiclassical approach

In this Appendix, in the $N = 3$ case, we provide an alternative approach to the conformal embedding one (15) to show the emergence of the $SU(3)_1$ critical phase in the phase diagram of the $SU(3)$ two-leg zigzag spin ladder (2) when $J_1 \ll J_2$.

Let us first consider the Euclidean action corresponding to Eq. (13):

$$\begin{aligned} \mathcal{S} &= \mathcal{S}[SU(3)_1; g_1] + \mathcal{S}[SU(3)_1; g_2] \\ &\quad + \lambda_1 \int d^2x \left[e^{i\pi/3} \text{Tr}(g_1 g_2^\dagger) + \text{H.c.} \right] \\ &\quad + \lambda_2 \int d^2x \left[e^{i\pi/3} \text{Tr} g_1 \text{Tr} g_2^\dagger + \text{H.c.} \right]. \end{aligned} \quad (\text{C1})$$

As already emphasized in section II B, the first term of Eq. (C1) with coupling constant λ_1 has a nonperturbative mass gap $\Delta \sim J_1^{N/2}$. The minimization of this term ($\lambda_1 > 0$) leads to $g_1 = -e^{-i\pi/3} g_2$, which is an $SU(3)$ matrix. We integrate out the g_1 degrees of freedom to deduce the effective action for $g_2 = G$:

$$\mathcal{S}_{\text{eff}} = \mathcal{S}[SU(3)_2; G] - 2\lambda_2 \int d^2x |\text{Tr} G|^2, \quad (\text{C2})$$

with $\lambda_2 < 0$ since $J_1 > 0$. The minimization of the action leads to the condition: $\text{Tr} G = 0$. The eigenvalues of the G matrix are the 3-rd roots of unity and the fundamental WZNW $SU(3)$ G field can be written as:

$$\begin{aligned} G &= U \Omega U^\dagger \\ \Omega &= \begin{pmatrix} 1 & 0 & 0 \\ 0 & \omega & 0 \\ 0 & 0 & \omega^2 \end{pmatrix}, \end{aligned} \quad (\text{C3})$$

U being a general $U(3)$ matrix and $\omega = e^{i2\pi/3}$. We then introduce 9 complex scalar fields Φ_{ij} ($i, j = 1, \dots, 3$) such that $U_{ij} = \Phi_{ij} = (\vec{\Phi}_j)_i$. These fields are constraint to be orthonormal complex vectors: $\vec{\Phi}_i^* \cdot \vec{\Phi}_j = \delta_{ij}$ to enforce the $U(3)$ property: $U^\dagger U = I$. The identification (C3) reads thus as follows in terms of the scalar fields:

$$G_{ij} = \sum_{a=1}^3 \Phi_{ja}^* \Omega_{aa} \Phi_{ia}. \quad (\text{C4})$$

A $U(1)^3$ redundancy in the description (C4) is manifest since the transformation $\vec{\Phi}_a \rightarrow e^{i\theta_a} \vec{\Phi}_a$ gives the same G_{ij} for all θ_a ($a = 1, 2, 3$). Distinct scalar fields take thus value in the manifold $U(3)/U(1)^3 \sim SU(3)/U(1)^2$, which is the flag manifold.⁸⁸

The next step of the approach is to replace the identification (C4) into the action (C2) to derive the low-energy effective field theory for the complex fields $\vec{\Phi}_i$. The action

takes the form of a nonlinear sigma model on the flag manifold $SU(3)/U(1)^2$ with topological θ terms with a Lagrangian density.^{89,90}

$$\begin{aligned} \mathcal{L} = & \frac{3}{4\pi} \sum_{a=1}^3 \left(|\partial_\mu \vec{\Phi}_a|^2 - |\vec{\Phi}_a^* \cdot \partial_\mu \vec{\Phi}_a|^2 \right) \\ & + \sum_{a=1}^3 \frac{\theta_a}{2\pi} \epsilon^{\mu\nu} \partial_\mu \vec{\Phi}_a^* \cdot \partial_\nu \vec{\Phi}_a \\ & + \sum_{1 \leq a < b \leq 3} (g_{ab} \delta^{\mu\nu} + b_{ab} \epsilon^{\mu\nu}) \left(\vec{\Phi}_a^* \cdot \partial_\mu \vec{\Phi}_b \right) \left(\vec{\Phi}_b^* \cdot \partial_\nu \vec{\Phi}_a \right), \end{aligned} \quad (\text{C5})$$

with $\theta_a = 4\pi a/3$ ($a = 1, 2, 3$), $g_{ab} = 3 \cos(2\pi(a-b)/3)/2\pi$ and $b_{ab} = 3 \sin(2\pi(a-b)/3)/2\pi$. Model (C5) contains three topological angles θ_a with topological charges:

$$q_a = \frac{i}{2\pi} \int d^2x \epsilon^{\mu\nu} \partial_\mu \vec{\Phi}_a^* \cdot \partial_\nu \vec{\Phi}_a \quad (\text{C6})$$

which are integers. However, the topological charges are not all independent due to the orthonormalization constraint: $\vec{\Phi}_i^* \cdot \vec{\Phi}_j = \delta_{ij}$ and satisfy: $\sum_{a=1}^3 q_a = 0$ since it can be shown $\sum_{a=1}^3 \vec{\Phi}_a^* \cdot \partial_\mu \vec{\Phi}_a = 0$.^{90,91} It implies that model (C5) is left invariant by shifting all topological angles by a same amount: $\theta_a \rightarrow \theta_a + \theta$ for all a . There are thus two independent topological angles $\theta_a = 4\pi a/3$ ($a = 1, 2$) in model (C5) in full agreement with the value of the second homotopy group for the flag manifold: $\Pi_2(SU(3)/U(1)^2) = \mathbb{Z} \times \mathbb{Z}$.⁹²

It has been shown recently that the flag sigma model (C5) with topological angles $\theta_a = 2\pi p a/3$ control the IR properties of $SU(3)$ Heisenberg spin chain in symmetric rank- p tensor representation in the large p limit.⁹¹ A gapless phase in the $SU(3)_1$ universality class has been predicted for model (C5) when p and 3 are coprime.^{89,90,93,94} In the particular $p = 2$ case, which share the same topological angles as in (C5), a large-scale DMRG calculation has shown the existence of a gapless $SU(3)_1$ behavior with central charge $c = 2$.⁸⁰ We thus conclude that the action (C1) describes a gapless behavior in the $SU(3)_1$ universality class. This leads to a second argument which shows that the two-leg $SU(3)$ zigzag spin ladder (2) displays a critical $SU(3)_1$ phase in the regime $J_1 \ll J_2$.

Appendix D: Additional numerical results

We discussed in the main text the scaling of the correlation length with the bond dimension in the different gapless phases. Fig. 14 presents the relevant data. We find that ξ does scale as χ^κ , but κ deviates from the predicted value⁸¹

$$\kappa = \frac{6}{c(\sqrt{\frac{12}{c} + 1})}. \quad (\text{D1})$$

In Fig. 15, we show the scaling of the incommensuration with the correlation length for the $SU(4)$ chain above $J_2 = 2$. We have not yet reached the scaling regime for the coherence length, though the incommensuration is largely converged.

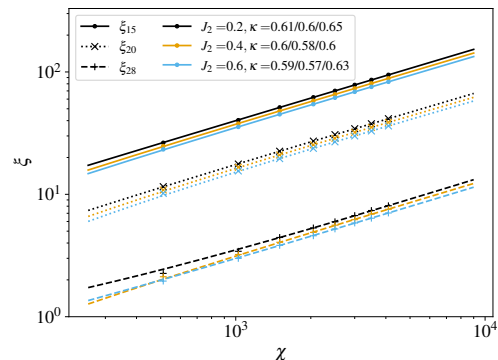
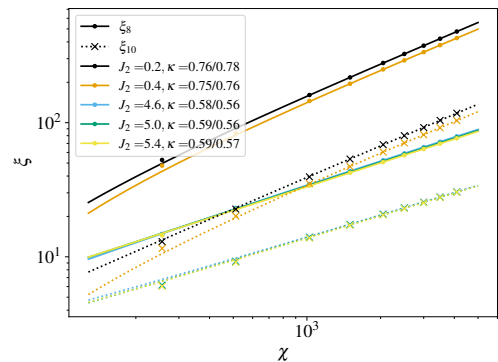


FIG. 14. Scaling of the dominant correlation length with the bond dimension for $SU(3)$ (top) and $SU(4)$ (bottom). In both cases, the exponents slightly deviate from the usual predictions.⁸¹

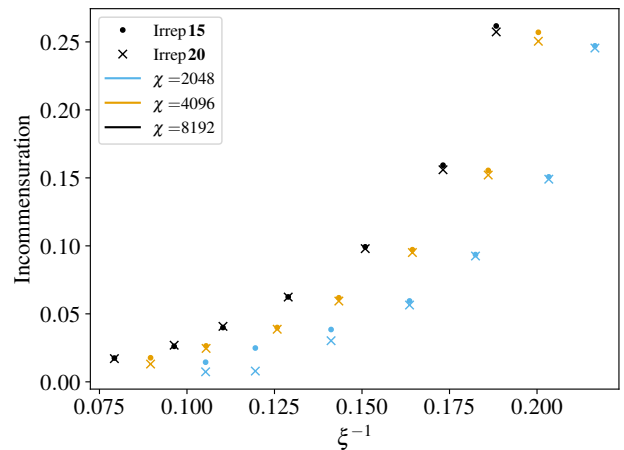


FIG. 15. Scaling of the incommensuration with the correlation length. We do not observe the linear behavior seen in the $SU(2)$ spin chain, though it could be due only to finite convergence.

Finally, in Fig. 16, we represent the connected correlations of the projector \hat{P}_{44} on the local state $(0, 0, 0, 1)$. The transition towards an incommensurate state at $J_2 \approx 2.0$ is directly visible in the oscillations of the exponentially decaying correlation functions, even though the corresponding

eigenvalues of the transfer matrix are subdominant.

Appendix E: SU(2) case

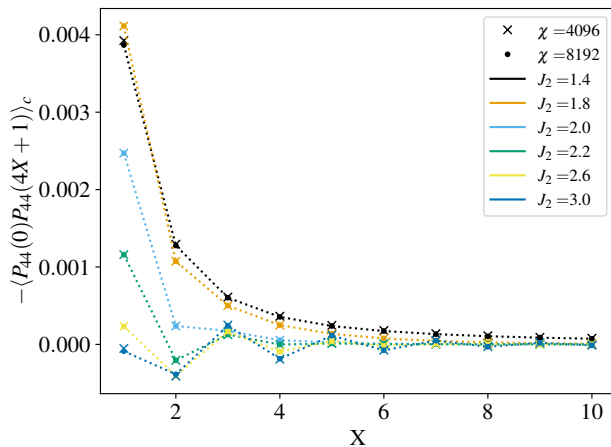


FIG. 16. Correlations of the projector \hat{P}_{44} on the fourth state of the local Hilbert space for different values of χ . The commensurate-incommensurate transition at $J_2 \approx 2.0$ is clearly visible.

For completeness, we review the well-studied case of SU(2) case, namely a spin-1/2 zigzag $J_1 - J_2$ chain. For $J_2 = 0$ this is the simple critical Heisenberg chain (with central charge $c = 1$). Using field-theory and exact diagonalization, the second-neighbour spin exchange opens a gap and a spontaneous dimerization appears when $J_2/J_1 \simeq 0.241167$, which can be found with high accuracy.⁹⁵ Then the dimerized phase persists for all larger J_2 couplings, including, in particular, the exact solution found by Majumdar and Ghosh²⁸ for $J_2/J_1 = 1/2$. For reference, Fig. 17 shows the measured dimerization obtained using iDMRG with relatively small bond dimensions. Quite interestingly, above this point, correlations become incommensurate³¹ with a pitch angle reminiscent of the classical model, as shown in Fig. 18.

- ¹ P. Anderson, *Mater. Res. Bull.* **8**, 153 (1973).
- ² L. Savary and L. Balents, *Rep. Prog. Phys.* **80**, 016502 (2016).
- ³ I. Affleck and J. B. Marston, *Phys. Rev. B* **37**, 3774 (1988).
- ⁴ N. Read and S. Sachdev, *Phys. Rev. Lett.* **62**, 1694 (1989).
- ⁵ C. Wu, *Mod. Phys. Lett. B* **20**, 1707 (2006).
- ⁶ M. Hermele and V. Gurarie, *Phys. Rev. B* **84**, 174441 (2011).
- ⁷ P. Corboz, M. Lajkó, A. M. Läuchli, K. Penc, and F. Mila, *Phys. Rev. X* **2**, 041013 (2012).
- ⁸ P. Nataf, M. Lajkó, A. Wietek, K. Penc, F. Mila, and A. M. Läuchli, *Phys. Rev. Lett.* **117**, 167202 (2016).
- ⁹ J.-Y. Chen, J.-W. Li, P. Nataf, S. Capponi, M. Mambrini, K. Totsuka, H.-H. Tu, A. Weichselbaum, J. von Delft, and D. Poilblanc, *Phys. Rev. B* **104**, 235104 (2021).
- ¹⁰ M. G. Yamada, M. Oshikawa, and G. Jackeli, *Phys. Rev. B* **104**, 224436 (2021).
- ¹¹ X.-P. Yao, Y. Gao, and G. Chen, *Phys. Rev. Research* **3**, 023138 (2021).
- ¹² H.-K. Jin, R.-Y. Sun, H.-H. Tu, and Y. Zhou, *Science Bulletin* **67**, 918 (2022).
- ¹³ H. Nonne, M. Moliner, S. Capponi, P. Lecheminant, and K. Totsuka, *Europhys. Lett.* **102**, 37008 (2013).
- ¹⁴ T. Morimoto, H. Ueda, T. Momoi, and A. Furusaki, *Phys. Rev. B* **90**, 235111 (2014).
- ¹⁵ V. Bois, S. Capponi, P. Lecheminant, M. Moliner, and K. Totsuka, *Phys. Rev. B* **91**, 075121 (2015).
- ¹⁶ S. Capponi, P. Lecheminant, and K. Totsuka, *Ann. Phys.* **367**, 50 (2016).
- ¹⁷ A. Roy and T. Quella, *Phys. Rev. B* **97**, 155148 (2018).
- ¹⁸ H. Ueda, T. Morimoto, and T. Momoi, *Phys. Rev. B* **98**, 045128 (2018).
- ¹⁹ P. Fromholz, S. Capponi, P. Lecheminant, D. J. Papoular, and K. Totsuka, *Phys. Rev. B* **99**, 054414 (2019).
- ²⁰ T. Zhang and G.-B. Jo, *Scientific Reports* **5**, 16044 (2015).

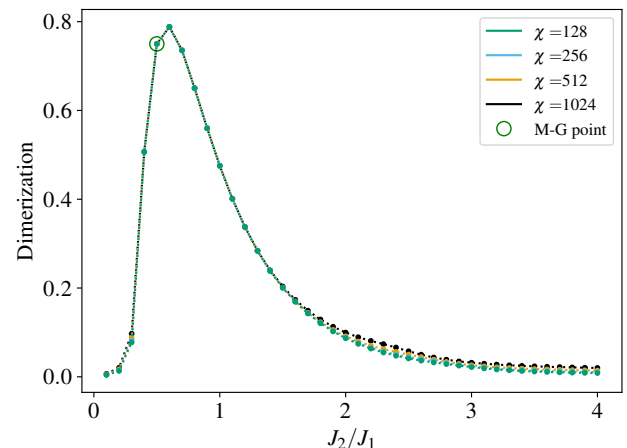


FIG. 17. Dimerization in the SU(2) $J_1 - J_2$ Heisenberg spin chain as a function of J_2/J_1 . At $J_2 \simeq 0.24$, a gapped dimerized phase opens. The exact product state described by Majumdar and Ghosh²⁸ is reached at $J_2 = 0.5J_1$. Small bond dimensions are enough to capture the physics of the chain.

- ²¹ S. Taie, R. Yamazaki, S. Sugawa, and Y. Takahashi, *Nat. Phys.* **8**, 825 (2012).
- ²² X. Zhang, M. Bishof, S. L. Bromley, C. V. Kraus, M. S. Safronova, P. Zoller, A. M. Rey, and J. Ye, *Science* **345**, 1467 (2014).
- ²³ G. Pagano, M. Mancini, G. Cappellini, P. Lombardi, F. Schafer, H. Hu, X.-J. Liu, J. Catani, C. Sias, M. Inguscio, and L. Fallani, *Nat. Phys.* **10**, 198 (2014).
- ²⁴ C. Hofrichter, L. Riegger, F. Scazza, M. Höfer, D. R. Fernandes, I. Bloch, and S. Fölling, *Phys. Rev. X* **6**, 021030 (2016).

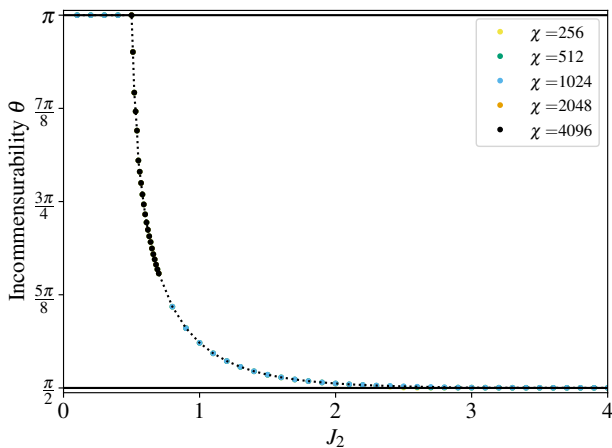


FIG. 18. Incommensurate angle for the $SU(2)$ J_1 - J_2 Heisenberg spin chain, measured as in Eq. (43). The incommensurability opens at the Majumdar-Ghosh point. Note that due to our unit cell, the angle is here defined modulo $\pi/2$. As we know that in the $J_2 = 0$ limit, the system is fully antiferromagnetic, we chose $\theta = \pi$ in the critical phase.

- 25 H. Ozawa, S. Taie, Y. Takasu, and Y. Takahashi, *Phys. Rev. Lett.* **121**, 225303 (2018).
- 26 S. Taie, E. Ibarra-García-Padilla, N. Nishizawa, Y. Takasu, Y. Kuno, H.-T. Wei, R. T. Scalettar, K. R. A. Hazzard, and Y. Takahashi, *Nat. Phys.* **18**, 1356 (2022).
- 27 F. D. M. Haldane, *Phys. Rev. B* **25**, 4925 (1982).
- 28 C. K. Majumdar and D. K. Ghosh, *J. Math. Phys.* **10**, 1388 (1969).
- 29 K. Okamoto and K. Nomura, *Phys. Lett. A* **169**, 433 (1992).
- 30 B. S. Shastry and B. Sutherland, *Phys. Rev. Lett.* **47**, 964 (1981).
- 31 S. R. White and I. Affleck, *Phys. Rev. B* **54**, 9862 (1996).
- 32 D. Allen and D. Sénéchal, *Phys. Rev. B* **55**, 299 (1997).
- 33 A. A. Nersesyan, A. O. Gogolin, and F. H. L. Eßler, *Phys. Rev. Lett.* **81**, 910 (1998).
- 34 C. Itoi and S. Qin, *Phys. Rev. B* **63**, 224423 (2001).
- 35 B. Sutherland, *Phys. Rev. B* **12**, 3795 (1975).
- 36 I. Affleck, *Nucl. Phys. B* **265**, 409 (1986).
- 37 I. Affleck, *Nucl. Phys. B* **305**, 582 (1988).
- 38 B. Frischmuth, F. Mila, and M. Troyer, *Phys. Rev. Lett.* **82**, 835 (1999).
- 39 R. Assaraf, P. Azaria, M. Caffarel, and P. Lecheminant, *Phys. Rev. B* **60**, 2299 (1999).
- 40 M. Führinger, S. Rachel, R. Thomale, M. Greiter, and P. Schmitteckert, *Annalen der Physik* **17**, 922 (2008).
- 41 M. Aguado, M. Asorey, E. Ercolessi, F. Ortolani, and S. Pasini, *Phys. Rev. B* **79**, 012408 (2009).
- 42 S. R. Manmana, K. R. A. Hazzard, G. Chen, A. E. Feiguin, and A. M. Rey, *Phys. Rev. A* **84**, 043601 (2011).
- 43 L. Messio and F. Mila, *Phys. Rev. Lett.* **109**, 205306 (2012).
- 44 J. Dufour, P. Nataf, and F. Mila, *Phys. Rev. B* **91**, 174427 (2015).
- 45 P. Nataf and F. Mila, *Phys. Rev. B* **97**, 134420 (2018).
- 46 H. Johannesson, *Nucl. Phys. B* **270**, 235 (1986).
- 47 P. Bouwknegt and K. Schoutens, *Nucl. Phys. B* **482**, 345 (1996).
- 48 D. Schuricht and M. Greiter, *Phys. Rev. B* **73**, 235105 (2006).
- 49 M. Greiter and S. Rachel, *Phys. Rev. B* **75**, 184441 (2007).
- 50 P. Corboz, A. M. Läuchli, K. Totsuka, and H. Tsunetsugu, *Phys. Rev. B* **76**, 220404 (2007).
- 51 M. Greiter, S. Rachel, and D. Schuricht, *Phys. Rev. B* **75**, 060401 (2007).
- 52 S. Rachel, R. Thomale, M. Führinger, P. Schmitteckert, and M. Greiter, *Phys. Rev. B* **80**, 180420 (2009).
- 53 I. Affleck, D. Gepner, H. Schulz, and T. Ziman, *J. Phys. A: Math. Gen.* **22**, 511 (1989).
- 54 C. Itoi and M.-H. Kato, *Phys. Rev. B* **55**, 8295 (1997).
- 55 K. Majumdar and M. Mukherjee, *J. Phys. A* **35**, L543 (2002).
- 56 A. J. A. James, R. M. Konik, P. Lecheminant, N. J. Robinson, and A. M. Tsvelik, *Rep. Prog. Phys.* **81**, 046002 (2018).
- 57 A. M. Tsvelik, *Sov. Phys. JETP* **66**, 754 (1987).
- 58 P. Lecheminant and A. M. Tsvelik, *Phys. Rev. B* **91**, 174407 (2015).
- 59 A. Gogolin, A. Nersesyan, and A. Tsvelik, *Bosonization and Strongly Correlated Systems* (Cambridge University Press, 1998).
- 60 A. Weichselbaum, S. Capponi, P. Lecheminant, A. M. Tsvelik, and A. M. Läuchli, *Phys. Rev. B* **98**, 085104 (2018).
- 61 S. Capponi, P. Fromholz, P. Lecheminant, and K. Totsuka, *Phys. Rev. B* **101**, 195121 (2020).
- 62 A. B. Zamolodchikov and V. Fateev, *Sov. Phys. JETP* **62**, 215 (1985).
- 63 P. Griffin and D. Nemeschansky, *Nucl. Phys. B* **323**, 545 (1989).
- 64 P. Di Francesco, P. Mathieu, and D. Sénéchal, *Conformal Field Theory* (Springer Verlag, 1996).
- 65 V. A. Fateev and A. B. Zamolodchikov, *Phys. Lett. B* **271**, 91 (1991).
- 66 V. Fateev, *Int. J. Mod. Phys. A* **6**, 2109 (1991).
- 67 P. Baseilhac and V. Fateev, *Nucl. Phys. B* **532**, 567 (1998).
- 68 P. Lecheminant, *Nucl. Phys. B* **901**, 510 (2015).
- 69 D. Gepner, *Nucl. Phys. B* **290**, 10 (1987).
- 70 K. Kikuchi, “RG flows from WZW models,” (2022), [arXiv:2212.13851](https://arxiv.org/abs/2212.13851).
- 71 P. Lecheminant, A. O. Gogolin, and A. A. Nersesyan, *Nucl. Phys. B* **639**, 502 (2002).
- 72 A. Vaezi and E.-A. Kim, “[Arxiv.1310.7434](https://arxiv.org/abs/1310.7434),” (2013).
- 73 G. Delfino and P. Grinza, *Nucl. Phys. B* **791**, 265 (2008).
- 74 V. G. Knizhnik and A. B. Zamolodchikov, *Nucl. Phys. B* **247**, 83 (1984).
- 75 M. Fishman, S. R. White, and E. M. Stoudenmire, *SciPost Phys. Codebases*, 4 (2022).
- 76 B. Vanhecke, J. Haegeman, K. Van Acoleyen, L. Vanderstraeten, and F. Verstraete, *Phys. Rev. Lett.* **123**, 250604 (2019).
- 77 P. Calabrese and J. Cardy, *Journal of Physics A: Mathematical and Theoretical* **42**, 504005 (2009).
- 78 We remind that the central charge for $SU(N)_k$ criticality is $c = k(N^2 - 1)/(k + N)$.
- 79 P. Nataf and F. Mila, *Phys. Rev. B* **93**, 155134 (2016).
- 80 P. Nataf, S. Gozel, and F. Mila, *Phys. Rev. B* **104**, L180411 (2021).
- 81 F. Pollmann, S. Mukerjee, A. M. Turner, and J. E. Moore, *Phys. Rev. Lett.* **102**, 255701 (2009).
- 82 S. Rachel and M. Greiter, *Phys. Rev. B* **78**, 134415 (2008).
- 83 L. Devos, L. Vanderstraeten, and F. Verstraete, *Phys. Rev. B* **106**, 155103 (2022).
- 84 Y. Fuji and P. Lecheminant, *Phys. Rev. B* **95**, 125130 (2017).
- 85 Y. K. Ha, *Phys. Rev. D* **29**, 1744 (1984).
- 86 E. Witten, *Comm. Math. Phys.* **92**, 455 (1984).
- 87 A. Polyakov and P. Wiegmann, *Phys. Lett. B* **141**, 223 (1984).
- 88 I. Affleck, D. Bykov, and K. Wamer, *Phys. Rep.* **953**, 1 (2022).
- 89 K. Ohmori, N. Seiberg, and S.-H. Shao, *SciPost Phys.* **6**, 17 (2019).
- 90 Y. Tanizaki and T. Sulejmanpasic, *Phys. Rev. B* **98**, 115126 (2018).

- ⁹¹ M. Lajkó, K. Wamer, F. Mila, and I. Affleck, *Nucl. Phys. B* **924**, 508 (2017).
- ⁹² D. Bykov, *Nucl. Phys. B* **855**, 100 (2012).
- ⁹³ K. Wamer and I. Affleck, *Phys. Rev. B* **101**, 245143 (2020).
- ⁹⁴ K. Wamer, M. Lajkó, F. Mila, and I. Affleck, *Nucl. Phys. B* **952**, 114932 (2020).
- ⁹⁵ S. Eggert, *Phys. Rev. B* **54**, R9612 (1996).